NAVAL POSTGRADUATE SCHOOL
Monterey, California

THESIS

DETONABILITY OF HYDROCARBON/AIR MIXTURES USING COMBUSTION ENHANCING GEOMETRIES FOR PULSE DETONATION ENGINES
by
Neil G. Sexton
June 2001
Thesis Advisor: Christopher M. Brophy
Co-Advisor: James V. Sanders
Second Reader: David W. Netzer

Approved for public release; distribution is unlimited.

REPORT DOCUMENTATION PAGE

Public reporting burden for this collection of information is estimated to average 1 hour per response, including the time for reviewing instruction, searching existing data sources, gathering and maintaining the data needed, and completing and reviewing the collection of information. Send comments regarding this burden estimate or any other aspect of this collection of information, including suggestions for reducing this burden, to Washington headquarters Services, Directorate for Information Operations and Reports, 1215 Jefferson Davis Highway, Suite 1204, Arlington, VA 22202-4302, and to the Office of Management and Budget, Paperwork Reduction Project (0704-0188) Washington DC 20503.

1. AGENCY USE ONLY *(Leave blank)*	2. REPORT DATE June 2001	3. REPORT TYPE AND DATES COVERED Master's Thesis

4. TITLE AND SUBTITLE **Detonability of Hydrocarbon/Air Mixtures Using Combustion Enhancing Geometries for Pulse Detonation Engines**	5. FUNDING NUMBERS Contract Number
6. AUTHOR(S) Sexton, Neil G.	N0001401WR20153

7. PERFORMING ORGANIZATION NAME(S) AND ADDRESS(ES) Naval Postgraduate School Monterey, CA 93943-5000	8. PERFORMING ORGANIZATION REPORT NUMBER

9. SPONSORING / MONITORING AGENCY NAME(S) AND ADDRESS(ES) Office of Naval Research Ballston Tower One 800 N. Quincy Street Arlington, VA 22217-5600	10. SPONSORING / MONITORING AGENCY REPORT NUMBER

11. SUPPLEMENTARY NOTES

The views expressed in this thesis are those of the author and do not reflect the official policy or position of the Department of Defense or the U.S. Government.

12a. DISTRIBUTION / AVAILABILITY STATEMENT Approved for public release; distribution unlimited.	12b. DISTRIBUTION CODE

13. ABSTRACT *(maximum 200 words)*

This research studied combustion enhancing geometries and shock reflection on generating a hydrocarbon/air detonation wave in a combustion tube. Ethylene was used as a baseline fuel to determine the preferable geometries. Propane was then used in later testing because of its combustion similarities with heavy hydrocarbon fuels such JP5, JP8, and JP10. Three criteria were used to measure the effectiveness of the combustion enhancing geometries: ability to generate a detonation, wave speed, and time for shock formation. The evaluated geometries included flow-restricting orifice plates and a Schelkin spiral. The shock reflection was accomplished by a vertical fence (large orifice) placed in the last fourth of the tube length. The optimum geometry was found to be the orifice plate used in conjunction with the spiral. Detonations occurred when using ethylene in this configuration, but did not develop when using propane. Because propane's overall reaction rate is slower than that of simpler fuels, more large- and small-scale turbulence to further enhance combustion needs to be generated to create a detonation wave in a short distance when using complex hydrocarbons, such as propane.

14. SUBJECT TERMS Detonation, Pulse Detonation Engine, Deflagration-to-Detonation Transition, DDT	15. NUMBER OF PAGES 88
	16. PRICE CODE

17. SECURITY CLASSIFICATION OF REPORT Unclassified	18. SECURITY CLASSIFICATION OF THIS PAGE Unclassified	19. SECURITY CLASSIFI- CATION OF ABSTRACT Unclassified	20. LIMITATION OF ABSTRACT UL

THIS PAGE INTENTIONALLY LEFT BLANK

DETONABILITY OF PROPANE/AIR AND ETHYLENE/AIR MIXTURES USING COMBUSTION ENHANCING GEOMETRIES FOR PULSE DETONATION ENGINE APPLICATIONS

Neil G. Sexton
Lieutenant, United States Navy
B.S., United States Naval Academy, 1995

Submitted in partial fulfillment of the
requirements for the degree of

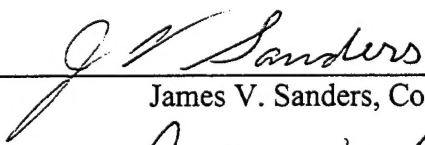**MASTER OF SCIENCE IN APPLIED PHYSICS**

from the

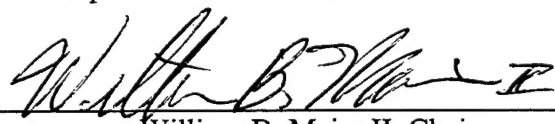**NAVAL POSTGRADUATE SCHOOL**
June 2001

Author: _____
Neil G. Sexton

Approved by: _____
Christopher M. Brophy, Thesis Advisor

_____
James V. Sanders, Co-Advisor

_____
David W. Netzer, Second Reader
Department of Aeronautics and Astronautics

_____
William B. Maier II, Chairman
Department of Physics

iii

THIS PAGE INTENTIONALLY LEFT BLANK

ABSTRACT

This research studied combustion enhancing geometries and shock reflection on generating a hydrocarbon/air detonation wave in a combustion tube. Ethylene was used as a baseline fuel to determine the preferable geometries. Propane was then used in later testing because of its combustion similarities with heavy hydrocarbon fuels such JP5, JP8, and JP10. Three criteria were used to measure the effectiveness of the combustion enhancing geometries: ability to generate a detonation, wave speed, and time for shock formation. The evaluated geometries included flow-restricting orifice plates and a Schelkin spiral. The shock reflection was accomplished by a vertical fence (large orifice) placed in the last fourth of the tube length. The optimum geometry was found to be the orifice plate used in conjunction with the spiral. Detonations occurred when using ethylene in this configuration, but did not develop when using propane. Because propane's overall reaction rate is slower than that of simpler fuels, more large- and small-scale turbulence to further enhance combustion needs to be generated to create a detonation wave in a short distance when using complex hydrocarbons, such as propane.

THIS PAGE INTENTIONALLY LEFT BLANK

TABLE OF CONTENTS

LIST OF FIGURES

THIS PAGE INTENTIONALLY LEFT BLANK

LIST OF TABLES

THIS PAGE INTENTIONALLY LEFT BLANK

LIST OF ABBREVIATIONS and SYMBOLS

A	Cross Sectional Area of Tube
$C\text{-}J$	Chapman Jouget Point
c	Local Sonic Velocity
E_a	Activation Energy
k	Reaction Rate
M	Mach number
$\dot{m}$	Mass Flow Rate
N	Number of Moles
p	Pressure
q	Total Heat Addition per Unit Mass
R_u	Gas Constant
T	Temperature
X_{ddt}	Deflagration-to-detonation transition distance
$1,2$	Subscripts identifying regions before and after combustion
γ	Ratio of Specific Heats at Constant Pressure and Volume
φ	Equivalence Ratio (see page 27)
ρ	Density
ν	Specific Volume $(1/\rho)$

THIS PAGE INTENTIONALLY LEFT BLANK

ACKNOWLEDGEMENTS

I would like to thank my thesis advisor, Dr. Chris Brophy, for his patience and effort in this project. I would also like to thank Dr. Jose Sinibaldi and Mr. Harry Conner for their help and support given throughout this endeavor.

Finally, I would like to thank my wife, Keiko, and daughter, Hana, for their understanding and endless encouragement.

THIS PAGE INTENTIONALLY LEFT BLANK

I.   INTRODUCTION

A.   BACKGROUND

There is a significant amount of research underway exploring Pulse Detonation Engine (PDE) technology. Once the nature of its operation is well understood, it is hoped that this type of engine would provide an alternative powerplant for aircraft or supersonic cruise missile propulsion. The combustion cycle in a PDE differs from most combustion engines because it relies on a detonative combustion process instead of a more commonly observed constant pressure combustion process. A detonation combustion process yields a higher thermal efficiency, and may eventually give a higher propulsion efficiency. [Ref. 1] Experimental results have shown that it is possible to achieve a detonation in a short distance, on the order of centimeters, by using a gaseous mixture of a hydrocarbon and oxygen in a combustion tube. [Ref. 2] One particular challenge of the PDE is to achieve a detonation reliably and within a distance practical for modern sized aircraft or missile engines using a gaseous hydrocarbon/air mixture with common jet fuels such as JP8 and JP5. To accomplish this, different methods of practical detonation initiation must be examined.

B.   OVERVIEW OF THIS RESEARCH

The goal of this research was to promote the rapid generation of a detonation wave by enhancing the turbulent mixing and subsequent combustion of the fuel-air reactants ignited by conventional spark ignition. A single-shot combustion tube was used to evaluate the effects of fuel/air ratios and different combustion enhancing geometries on producing a detonation wave in a fuel/air mixture. The results are more quantitative than

1

in a fully operational PDE because the well operation of the tube and facility were well controlled.

Many studies have been performed to investigate how to increase turbulent mixing using fence-like obstacles placed within a combustor tube [Ref. 3] or by using a rough-walled tube [Ref. 4]. This research investigated two methods of increasing turbulent mixing and combustion. The first was a spiral lying along the wall of the tube. The second was an orifice plate to vent the combustion products. A vertical fence was also used to reflect the generated shock and increase the temperature of the unburned reactants. It was hoped that the reflected shock would increase the temperature of the remaining reactants to auto-ignition and lead to a detonation. The physics of this process will be discussed in a later section.

A substantial amount of fundamental PDE research has been done with simple fuels such as hydrogen, acetylene, and ethylene. A great deal more needs to be performed on more complex liquid fuels similar to those found in modern propulsion systems and which posses a much higher energy density. Additionally, air is the sensible oxidizer to use since carrying oxygen for combustion on a propulsion system would require extra weight and expense. The difficulty of achieving a detonation with heavy hydrocarbon fuels and air has been well documented. [Ref. 5] The energy required to directly form a detonation in a complex hydrocarbon is about 100 kJ, which equates to about 25 g of high explosive. [Ref. 5] Supplying such large amounts of energy through explosives is impractical due to its inherent danger and structural limitations on aircraft.

This research investigated the detonation properties of both ethylene (C_2H_4) and propane (C_3H_8) with air in a tube with various turbulence generating geometries and

initial conditions. Ethylene was used as the baseline fuel to determine potential geometries that would work when used with propane. Propane was chosen as the second fuel because its combustion properties are similar to more complicated hydrocarbons such as JP8 and JP5. Therefore, it allowed the careful study of complicated initiation problems associated with the more complex fuels without dealing with the atomization and vaporization issues of these liquid fuels.

THIS PAGE INTENTIONALLY LEFT BLANK

II.   THEORY

A.   INTRODUCTION

Three basic definitions are used to describe combustion events: deflagration, detonation, and explosion. Most people are generally familiar with the effects of an explosion. An explosion is a rapid expansion of gases from a confined space, but does not necessarily require a combustion wave traveling through those gases. The rapid expansion is usually due to the structural failure of the confining medium.

In a deflagration, a subsonic combustion wave travels into a medium of unburned reactants. Since the wave is subsonic, there is very little pressure change across the combustion wave. Some common examples of a deflagration include the combustion in a candle flame, a gas turbine engine, and a flame moving over an open gasoline spill. Deflagration flame speeds typically range from 1 m/s to 30 m/s.

In a detonation, a supersonic combustion wave propagates into a combustible medium. These conditions will be discussed in the next section. A detonation is a very violent and rapid event with pressures and temperatures much higher than in a deflagration. Pressure ratios across a detonation wave in gaseous hydrocarbon and air mixtures are as high as 30:1.

B.   THERMODYNAMICS OF DEFLAGRATIONS AND DETONATIONS

1.   Difference Between Deflagrations and Detonations

The theory to describe deflagrations and detonations is based on a one-dimensional model developed at the beginning of the 1900's. Detonations were discovered and described in 1873 by F.A. Abel. [Ref. 6] In 1901, Two scientists, D.

5

Chapman and E. Jouguet separately developed matching theories, now known as the Chapman-Jouguet theory, which describe the thermodynamic properties of a one-dimensional detonation wave. One unique aspect of this theory is that only the initial pressure and specific volume of the gas must be known to predict detonation wave speed and final pressure and specific volume. The Chapman-Jouguet (C-J) theory predicts the properties of three dimensional detonation wave speeds to within experimental uncertainty. [Ref. 7]
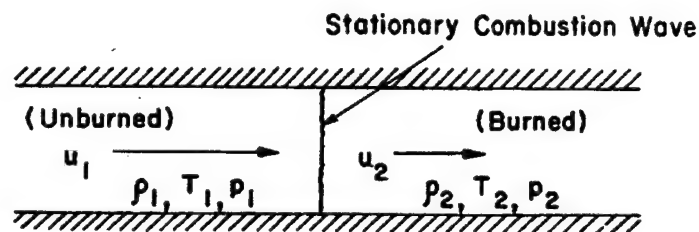
Figure 2-1. Schematic of Stationary 1-D Combustion Wave. [From Ref. 7]

It is helpful to set a reference frame moving with the combustion wave to describe events taking place inside a combustion tube (Figure 2-1). In this frame, the unburned reactants move toward the stationary combustion wave at velocity u_1. The burned reactants move away from the combustion wave at velocity u_2. There is a very large difference between these two velocities depending on whether the combustion wave is due to deflagration or detonation. This difference is explained by C-J theory. Table 2-1 below compares some values of deflagration and detonation properties. The terms c, T, ρ are local sonic velocity, temperature and density respectively.

Table 2-1. Qualitative Difference Between Detonation and Deflagration. [From Ref. 7]

Properties	Deflagration	Detonation
u_1/c_1	0.0001 - 0.03	5 – 10
u_2/u_1	4 - 6 (acceleration)	0.4 - 0.7 (deceleration)
p_2/p_1	$\cong$ 0.98 (slight expansion)	13 - 55 (compression)
T_2/T_1	4 - 16 (heat addition)	8 - 21 (heat addition)
ρ_2/ρ_1	0.06 - 0.25	1.7 - 2.6

2.   The Hugoniot Curve and the Chapman-Jouguet Points

The Hugoniot curve (Figure 2-2) graphs the solutions to a combustion event in a constant area combustor as pressure versus specific volume. A thorough derivation of the Hugoniot curve may be found in Kuo, [Ref. 7] and thesis work by Robinson [Ref. 1]. The derivation uses the conservation equations of continuity, momentum, and energy. It also assumes steady, adiabatic, one-dimensional flow in a constant volume combustor. The final equation takes the form

$$\frac{\gamma}{\gamma-1}\left(\frac{p_2}{\rho_2}-\frac{p_1}{\rho_1}\right)-1/2(p_2-p_1)\left(\frac{1}{\rho_1}+\frac{1}{\rho_2}\right)=q \qquad [2-1]$$

where q is the heat addition per unit mass of the reactants. The initial pressure and density, p_1 and ρ_1, are known before the reaction. The ratio of the specific heats at constant volume and pressure, γ, may be found in gas tables for the mixture. The resultant pressure, p_2, can be found by solving for a range of $\dfrac{1}{\rho_2}$ or vice versa.
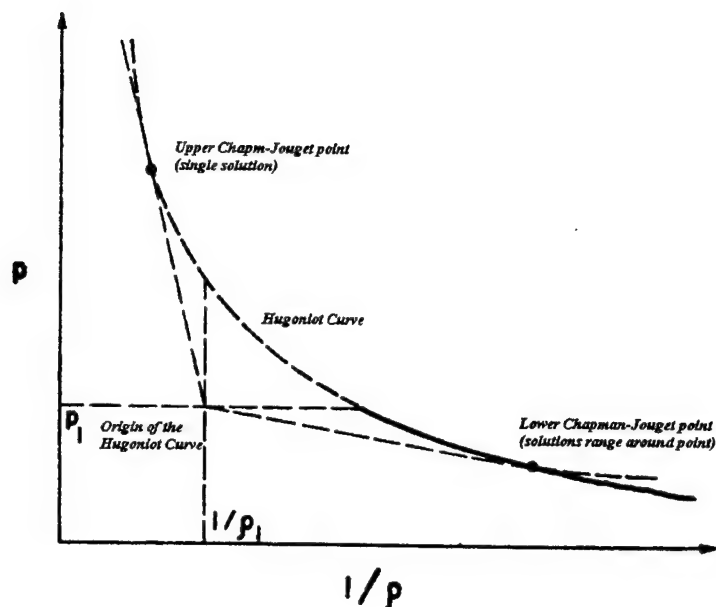
Figure 2-2. Physical Solutions to the Hugoniot Equation. [From Ref. 2]

As the amount of heat addition increases (a more energetic mixture of reactants) the Hugoniot curve moves up and to the right. The opposite occurs if q is decreased for a particular mixture.

The different regions of the Hugoniot curve are shown in Figure 2-3. These represent different aspects of a combustion event. Region V can be set aside since no physical solutions can exist there. The reason for this is that the speed of the unburned reactants mathematically is an imaginary number in region V.

8

Figure 2-3. Different Sections of the Hugoniot Curve. [From Ref. 2]

The C-J points, defined by Chapman and Jouguet, mark the separation of regions

I and II and regions III and IV. These points are called upper C-J and lower C-J, and are

labeled U and L respectively. The C-J points may be found by drawing straight lines

from the initial point $(p_1, \dfrac{1}{\rho_1})$ to two points tangent to the Hugoniot curve. These

straight lines are known as Rayleigh lines and represent the limitation that the post

combustion flow velocity cannot accelerate past Mach 1 in a constant area combustion
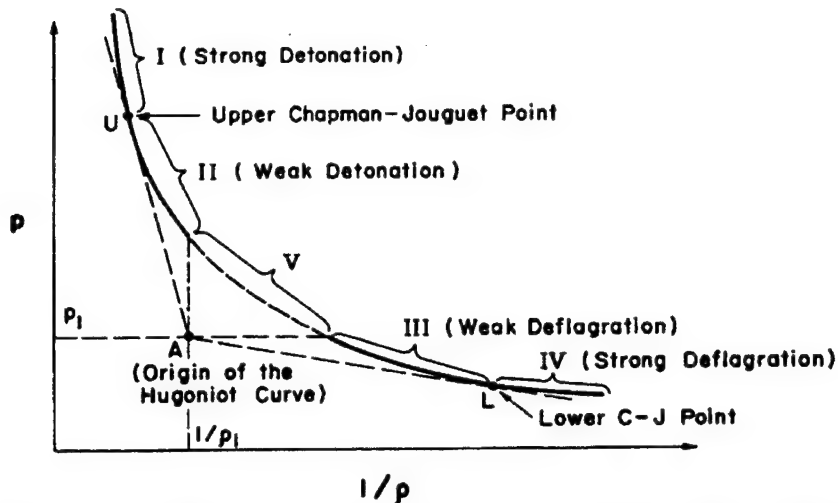
tube. Also counterintuitive is the fact that adding heat to an already supersonic flow will

slowly force it back towards Mach 1. A detailed explanation of the Rayleigh limit may

be found in Zucker. [Ref. 8]

If one manipulates the Hugoniot relationships and solves for the wave speed

ahead of a detonation wave in the laboratory reference frame at U, it is found to be highly

supersonic (Mach>5). This solution is associated with the upper C-J point. If the wave

becomes overdriven and its velocity exceeds this speed, p_2 and ρ_2 can only be in region I

for a short time, quickly falling back to the thermodynamic stability corresponding to the

9

pressure and specific volume found at U. Therefore, region I is called the 'strong detonation' region which indicates the pressure and density of the burned gases are higher than the values at U.

Region II is called the weak detonation region. Here, the pressure of the burned gases is also more than that of the unburned gases. As mentioned previously, region I may be obtained for a short period, but region II requires special circumstances regarding the reactant's chemical kinetics and is hard to achieve in the laboratory or in nature. If a reaction is to be in region II, its kinetics must be such that the reaction is occurring everywhere at the same time within the gas confinement. An almost instant reaction is the only way enough heat can be released fast enough to drive the reaction to region II during its path to U. Additional detail regarding the paths from initial pressure and density to U will be discussed in the Chemical Kinetics paragraph.

All developed detonations observed have the properties closely associated with the upper C-J point and the velocity of the gases behind the shock front, u_2, are sonic (M=1). The fact that flow behind the detonation wave is sonic can be seen by the following derivation. Differentiate Equation 2-1 with respect to ρ_2 and apply the fact that the Rayleigh lines and Hugoniot curve intersect at U and L:

$$\frac{P_2 - P_1}{\left(\dfrac{1}{\rho_2} - \dfrac{1}{\rho_1}\right)} = -\gamma P_2 \rho_2 \qquad [2\text{-}2]$$

Then take the continuity equation

$$\dot{m} = \rho_1 u_1 A_1 = \rho_2 u_2 A_2 \qquad [2\text{-}3]$$

and the momentum equation

$$P_1 + \rho_1 u_1{}^2 = P_2 + \rho_2 u_2{}^2 \qquad\qquad [2\text{-}4]$$

and combine them and set equal to Equation 2-2. The result is

$$u_2{}^2 = \frac{\gamma P_2}{\rho_2} = c_2{}^2, \quad |u_2| = c_2. \qquad\qquad [2\text{-}5]$$

Region III describes weak deflagrations. The velocity of the combustion products is accelerated here, but is still subsonic. This is the category into which almost all deflagrations fall. The lower C-J point, L, marks the speed limit for deflagration events. Anything in region IV is impossible since flow cannot change from subsonic to supersonic in a constant area duct due to the Rayleigh conditions previously mentioned.

3. Wave Structure

In the early 1940' s Zeldovich, von Neumann, and Doring independently arrived at a theory of detonation wave structure. Figure 2-4 will help in the explanation of this theory. The detonation wave is lead by a shock wave traveling at the detonation speed. Immediately after the shock wave, the reactants do not combust, but are heated. The pressure, density, and temperature rise sharply as the shock passes. This is followed by an area called the induction zone where the chemical reactants are heated and remain at a somewhat constant temperature. Eventually (~ 1 μs), the reactants begin to interact at a faster rate as the temperature dramatically increases. The temperature rises exponentially but the pressure and density fall because the volume behind the shock wave continues to increase as the shock wave moves down the tube causing the gases behind it to expand.
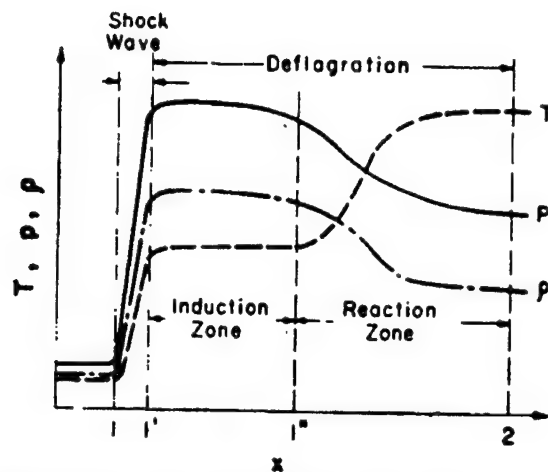
Figure 2-4. ZND Model of a Detonation Wave Structure. [From Ref. 7]

4.   Chemical Kinetics

In the beginning of this chapter it was stated that, with initial conditions of p_1 and ρ_1, fully developed detonations end up at the upper C-J point U on the Hugoniot curve. In nature, however, detonations do not follow a thermodynamic path from the center of the Hugoniot curve directly to the upper C-J point (path 'a' in Figure 2-5). Path 'd' indicates there is no chemical heat release until very late in the compression mode, where the heat release results in the path ending up on the final Hugoniot curve. In nature, the path a detonation takes is somewhere between 'b' and 'c', which is indicative of a finite heat release rate. The path the detonation takes to reach U depends upon how fast the chemical reaction between the fuel and oxidizer takes place.

It has been shown that chemical kinetics follow the Arrhenius rate law (Equation 2-6) and that reaction rates increase with increased temperature. Faster chemical kinetics results in a more rapid energy release which then results in the generation of a shock wave and then finally into a steady state detonation wave.

12

The von Neumann spike, commonly observed at the leading edge of a detonation wave, occurs due to the extremely high pressures associated with the deflagration-to-detonation transition. The high pressures and temperatures quickly fall to the point U and will be described in the next paragraph.
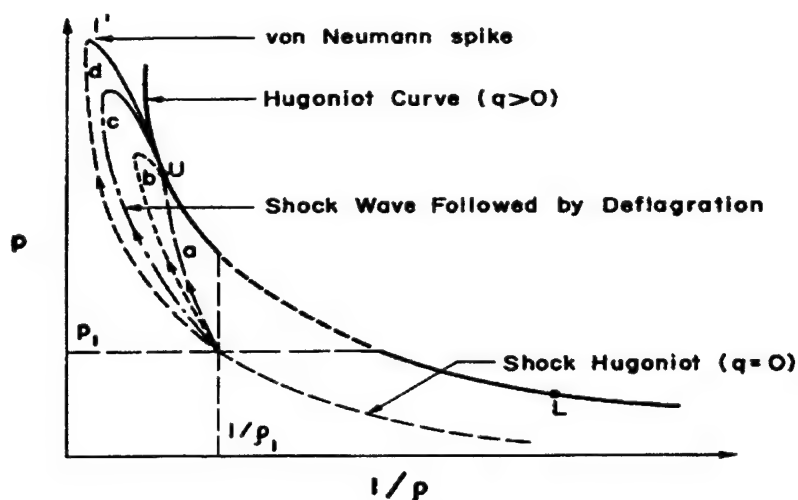
Figure 2-5. Paths to Detonation. [From Ref. 7]

The Arrhenius rate law is defined as

$$k = A \exp\left(\frac{-E_a}{R_u T}\right). \qquad [2-6]$$

The term 'k' is the rate of the reaction and 'A' is a constant specific to each chemical reaction. The activation energy is denoted E_a and R_u is the universal gas constant. Temperature T is in the denominator of the exponential, therefore the reaction rate increases exponentially as the temperature increases.

5. Development of a Detonation Wave

Detonations can be initiated in one of two ways: direct-ignition and thermal-ignition. Direct ignition takes place, for example, when explosives are used to create

strong shock waves in a tube filled with a combustible mixture that immediately turn into detonation waves.

Thermal-ignition occurs when a gaseous mixture of fuel and oxidizer are ignited and the combustion wave accelerates until conditions allow a detonation to be formed. The process of transforming a deflagration wave, which most combustion events are, to a detonation is called a deflagration-to-detonation transition. The distance in which this event occurs is often called the deflagration-to-detonation transition distance and is abbreviated X_{ddt}. The process for deflagration-to-detonation transition is very complicated and is explained in an example below.

The thermal-ignition method is studied in this thesis work since it is more suitable for aircraft and missile propulsion. The following section will discuss qualitatively how a simple tube filled with a combustible mixture of a fuel and oxidizer once ignited by a conventional ignition system, will transform from a deflagration into a detonation. Figure 2-6 is a series of schlieren images taken of a deflagration-to-detonation transition and will be referenced in this description. [Ref. 7]

Assume a tube is filled with a combustible mixture. One end of the tube is closed and one end open. The ignition source can be an automotive spark plug that ignites the mixture at the closed end of the tube. The combustion wave initially propagates as a laminar flame front which would rapidly transition into a turbulent flame front. This flame front propagates at 5-10 times that of the laminar speed. Traveling toward the open end of the tube at a speed on the order of 10 m/s, this flame front sends out weak compression waves which propagate towards the open end at the local sonic velocity
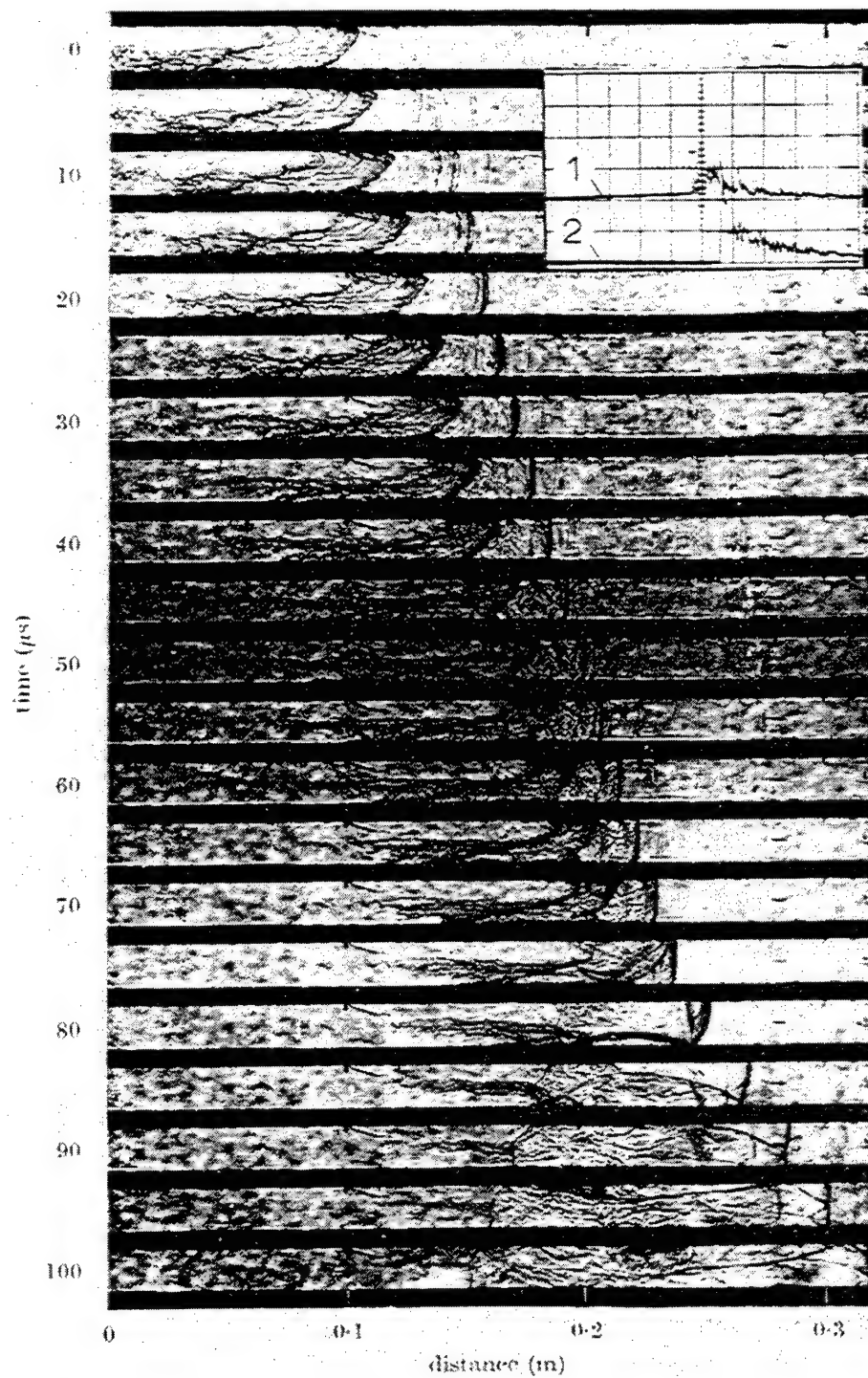
14

Figure 2-6. Deflagration-to-Detonation Transition. [From Ref. 7]

(Figure 2-6, 0- 10 µs). The temperature of the unreacted mixture rises slightly each time a compression wave passes which raises the local sound velocity.

Local sonic velocity is defined by the expression

$$c = \sqrt{\gamma R T} \, .$$

[2-7]

The ratio of the specific heats, γ, can be found for both the reactants and hot products throughout a reaction. The gas constant, R, is dependent on the molecular weight of the gas and T is the local temperature. As these compression waves coalesce a shock wave develops (Figure 2-6, ~35 µs).

The increased temperature behind the shock serves to increase the sonic velocity even higher still. The turbulent flame front continues to accelerate as it passes through the pre-heated and pressurized gases, creating a combustion driven shock. The combustion wave is still sending compression waves toward the shock and the temperature within the zone continues to rise. Eventually there will be enough energy between the shock and the combustion front that an explosion will occur among the unburned reactants (Figure 2-6, 75 µs). This violent event sends strong secondary shock waves in all directions and ultimately allows the combustion zone to occur immediately after the leading shock wave. A detonation wave will result which propagates at a supersonic velocity.

The detonation sends out extremely strong shock waves toward both the open and closed ends of the tube. The shock front that was traveling around 450 m/s, or about Mach 1.4, is now traveling at about 1800 m/s, or about Mach 5 relative to the unburned reactants. The reaction zone is now immediately behind the leading shock of the detonation wave because the reactants in the reaction zone have been consumed.

16

Interestingly, the detonation wave does not degenerate because it is now being sustained by the rapid combustion zone (Figure 2-6, 100 μs).

As the detonation shock wave passes through the unburned reactants, they are preheated to an extremely high temperature. The equations governing the temperature ratios before and after a shock in a perfect gas are:

$$M_2{}^2 = \frac{M_1{}^2 + \dfrac{2}{(\gamma-1)}}{\left(\dfrac{2\gamma}{\gamma-1}\right)M_1{}^2 - 1}, \qquad [2\text{-}8]$$

and

$$\frac{T_2}{T_1} = \frac{1 + \dfrac{(\gamma-1)}{2}M_1{}^2}{1 + \dfrac{(\gamma-1)}{2}M_2{}^2}. \qquad [2\text{-}9]$$

Both M_2 and T_2/T_1 are tabulated in most thermodynamics texts and can be found quickly. For example, if the temperature inside the tube, T_1, is 290 K and a shock wave is traveling at M_1=5, then the temperature after the shock has passed, T_2, is calculated to be 1682 K before any heat is released by the reactants, where $\gamma = 1.4$, typical for air, has been used.

The reaction zone behind the shock front is on the order of 1-2 cm thick. The reactants combust almost immediately after the shock has passed which keeps the flame front close to the shock front and support it with its compression waves still traveling forward at the sonic velocity.

The simplified model just presented, however, does not explain everything that is taking place in a deflagration to detonation transition. The above-mentioned events take a finite amount of time to occur. Most deflagrations can transition to a detonation if they are partially confined, as in a tube, and given enough tube length. Typical X_{ddt} lengths

for most hydrocarbon/air combustion range from 5 to 10 meters in a smooth tube with no obstacles or turbulence inducing geometries. Practical lengths for propulsion purposes are about 1 m which means that X_{ddt} must take place within about 0.3 m. The question that arises is how to make X_{ddt} shorter and more predictable. One method to decrease X_{ddt} is through increasing the overall reaction rate by increasing the initial mixture temperature which will accelerate the flame speed and also increase the temperature across the normal shock

6.   Increasing Reaction Rate Through Turbulence

The above example shows that the compression waves heat the unburned reactants ahead of the combustion wave and that this process is continually occurring as the flame front continues to accelerate toward the shock front. It is well known that hot gas jets injected into unburned reactants rapidly increase the overall reaction rate and accelerate the resulting flame faster than a laminar flame front because of the turbulent mixing. [Ref. 9] Part of this research was to investigate the effects of using hot jets emitted through an orifice plate with symmetrically placed holes. Several different orifice geometries were tried with varying total venting areas.

The simple combustion tube example can be altered by adding a reservoir chamber from which hot combustion products exit. The process begins by filling both combustion chamber and tube with a gaseous mixture of a hydrocarbon and air. The igniter is placed at the head-end of the reservoir so that the mixture begins to react there first. As will be shown in the Results Section, the pressure rises in the reservoir causing a pressure differential which results in a flow into the combustion tube. The flow from the

confined chamber into the tube is composed of very hot combustion products which then ignite the mixture immediately downstream of the plate.

7. Increasing Temperature Through Shock Reflection

The shock reflection procedure was applied in conjunction with the combustion chamber providing hot gas jets. The concept is based upon the shock generating capability of the orifice plate geometry. Shock reflection is achieved by a simple disk partially blocking flow downstream of the combustion chamber, called a fence. Previously it was stated that the static temperature increases after a shock passes. If a shock passes unburned reactants and is reflected to pass back over those same reactants, albeit in the reverse direction, the temperature again rises.

The shock reflection plate allows the middle 80% of the shock wave to travel through and the remaining 20% to reflect back into the already compressed and heated reactants. It was hoped that the increased temperature would cause the mixture between the shock front and the flame front (induction zone and reaction zone in Figure 2-4) to reach its auto-ignition temperature and detonate.

THIS PAGE INTENTIONALLY LEFT BLANK

III. EXPERIMENTAL SETUP AND PROCEDURE

A. INTRODUCTION

The testing facility was located at the Rocket Propulsion and Combustion Laboratory at the Naval Postgraduate School in Monterey, California. The experimental hardware (Figure 3-1) consisted of a segmented combustion tube, optical section, combustion chamber, orifice plate, variable ignition system, control valves, mixing tank, and high speed pressure transducers. The control valves, ignition system, and data acquisition were controlled remotely by a Visual Basic Graphic User Interface (GUI) code developed specifically for this testing. Initial conditions, desired fuel ratios, and other information were entered into the control program prior to a run.
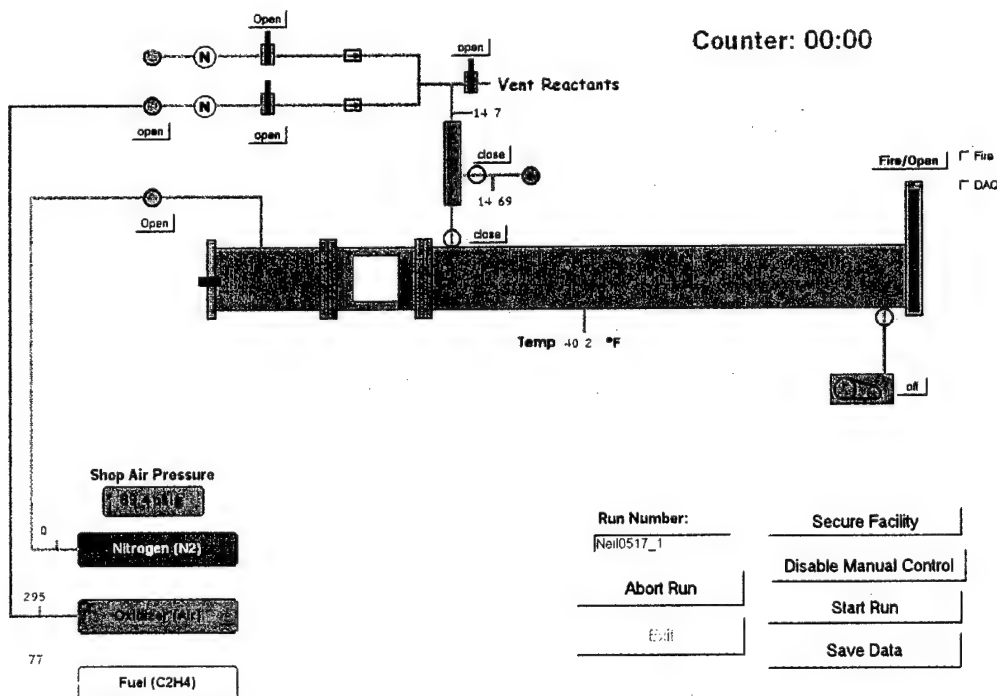

Figure 3-1. Visual Basic GUI Code to Remotely Control Operations.

Runs could be conducted automatically or in manual mode. The control to fire the spark plug had to be performed manually in either mode to ensure the highest level of safety. A test run could be aborted at any time and the reactants vented if a dangerous situation arose. A listing of the Standard Operating Procedure for operation of the facility is shown in Figure A-14.

B. HARDWARE DESCRIPTION AND FUNCTIONS

1. Combustor Tube

The combustor tube was one of the most important pieces of hardware. Two tubes were used in this experiment. The first tube was the baseline tube and had an inner diameter (ID) of 10.16 cm (4 in) and length of 134.6 cm (53 in). The tube was made of type-316 stainless steel and had 9 tapped ports for high-speed pressure transducers, fuel/air mixture line, vacuum pump, and a low speed pressure transducer line. There were flange assemblies at each end to connect to the combustor/optical section and the diaphragm/end-valve when drawing a vacuum. The baseline tube was used to determine the best orifice plate geometry, effect of initial tube pressure on the ignition characteristics, and the effect of the equivalence ratio of the reactants. An additional configuration allowed the reflection fence to be placed at the end of the tube, followed by a shorter tube.
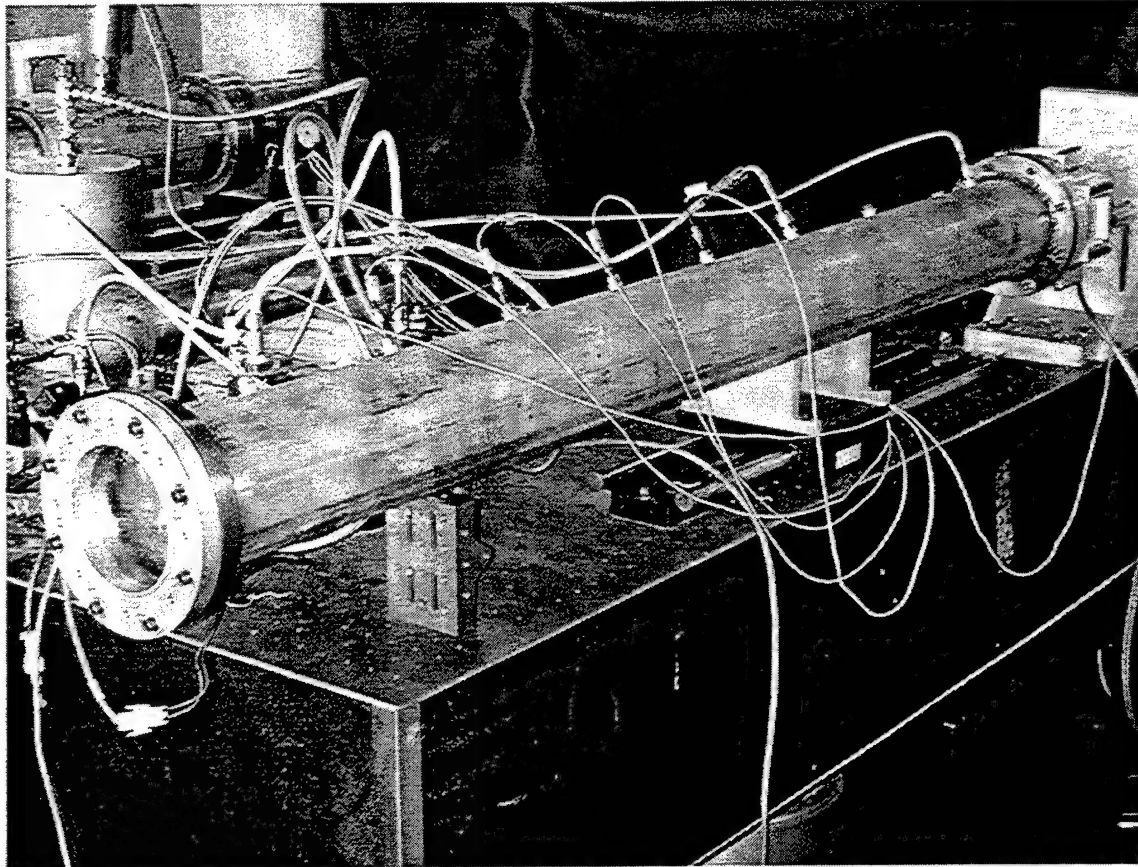
Figure 3-2. Baseline Tube Showing High-Speed Pressure Transducer Placement.

2.   Optical/Combustion Section

The stainless steel optical-access section was also a segment of the combustion

chamber in the baseline tube. There were four ports in the optical section for viewing

events in that section and it was used to view the initial combustion kernel growth, orifice

plate venting, or shock formation depending on axial placement of the section. When

imaging was desired, a quartz window was placed over a particular port and held in place

with a bracket. If imaging was not required, aluminum blanks were placed over the ports.
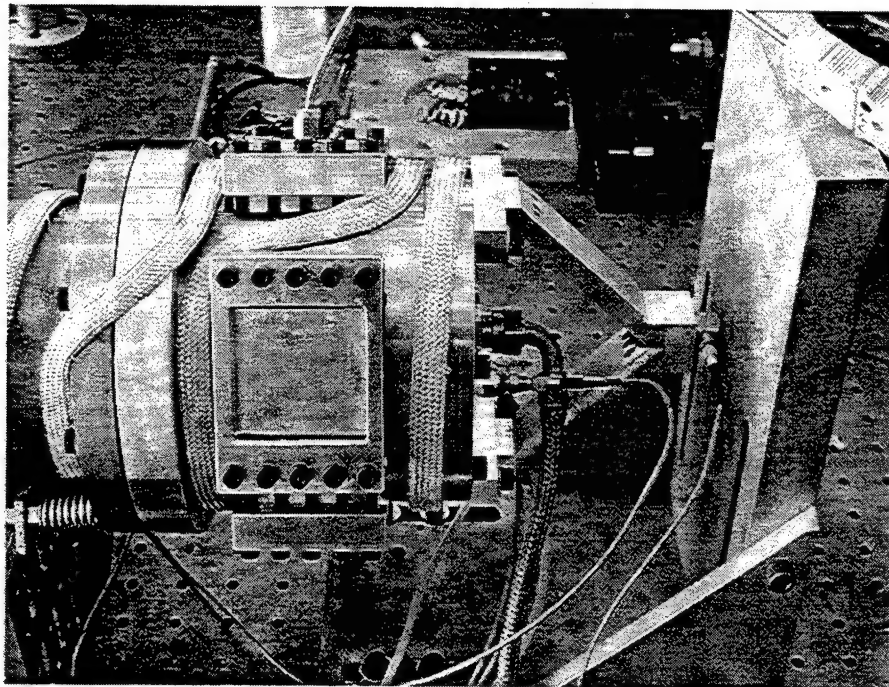
23

Figure 3-3. Optical section, Located at Head-End of Tube.
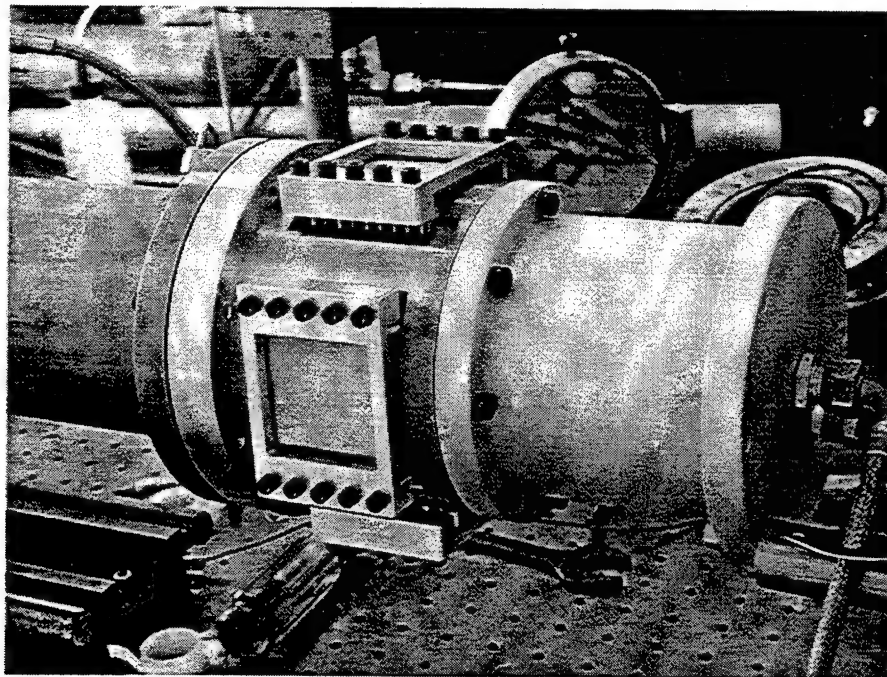

Figure 3-4. Setup to Image Jet Venting.

3. Orifice Plates

Orifice plates were stainless steel or aluminum round discs with circular holes of varying size symmetrically drilled into them. The orifice plates provided escape holes for the hot combustion products in the reservoir section. The combustion products vented into the main tube section resulting in the rapid mixing and combustion of the unburned reactants in the main tube.

Table 3-1. Orifice Plate and Wire Mesh Sizes.

	7-Hole	24-Hole Plate 1	24-Hole Plate 2	24-Hole Plate 3	24-Hole Plate 4	Wire Mesh
Hole dia.	0.2997 cm	0.1499 cm	0.2410 cm	0.2997 cm	0.4216 cm	0.1016 cm
Total Venting Area	0.494 sq cm	0.423 sq cm	1.095 sq cm	1.693 sq cm	3.351 sq cm	40.537 sq cm

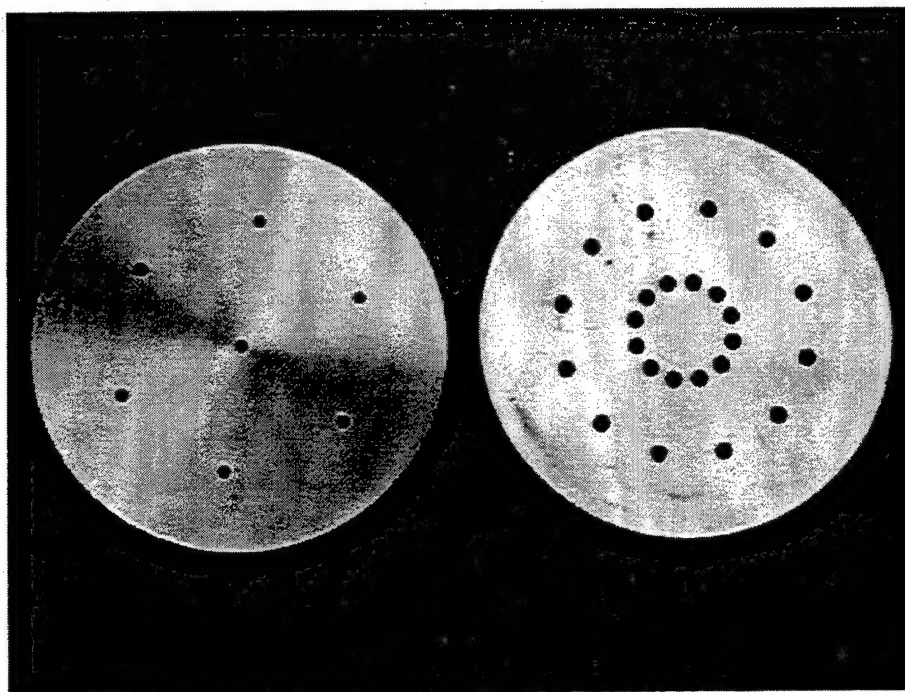Figure 3-5. 7-Hole and 24-Hole Orifice Plates.

4. Ignition System

The ignition system was a Unison Vision-2 Variable Ignition System (VIS-2) capacitive discharge system which used a Champion aircraft igniter. The VIS-2 igniter energy delivery can be varied from 0.070 to 2.03 Joules. The VIS-2 was set to deliver 2.03 Joules throughout this testing.

5. Mixing Tanks

The mixing tanks consisted of two tanks connected in parallel to increase the volume and decrease the required pressure to fill the combustion tube. The mixing tanks needed to be pressurized to 3.3 atmospheres (atm) for every 1.0 atm in the combustion tube. The mixing tanks were filled with the proper fuel and oxidizer partial pressures according the desired equivalence ratio, which was an input parameter in the Visual Basic control program. The mixing tanks and combustion tube were first taken to a vacuum pressure of 0.10 psia before fuel and air were injected. Once the proper vacuum pressure was reached a ball valve closed to separate the combustion tube from the mixing tanks. A ball valve and solenoid valve, which provided double valve protection, were then opened to allow fuel to flow into the mixing tanks. Needle valves were used to control fuel and oxidizer flow rate. Once the fuel partial pressure was met, the fuel valves would close and the oxidizer valves would open until the total pressure required was reached.

The mixture of fuel and oxidizer was allowed to stand between 2 and 5 minutes, depending on mixing tank pressure, to mix thoroughly before being injected into the combustion tube.

6.   Filling the Mixing Tanks

This testing was done with ethylene and propane as fuels, and air as the oxidizer. It was necessary to determine combustion properties of both lean and rich gaseous mixtures. The gases were injected into the mixing tanks according to the desired equivalence ratio, φ, set before the test run. Equivalence ratio is defined as

$$\varphi = \frac{N_f / N_o}{\left(N_f / N_o\right)_{ST}}. \qquad [3\text{-}1]$$

The term N is the moles of fuel or oxidizer. The subscript 'ST' denotes the stoichiometric ($\varphi = 1.0$) ratio of fuel to oxidizer. Stoichiometric combustion occurs when there is no excess fuel or oxidizer remaining in the products. If it is desired to fill the mixing tanks to 1 atmosphere with a fuel rich equivalence ratio of $\varphi = 1.4$, the partial pressures of fuel and oxidizer must be found.

The partial pressures of fuel and oxidizer for the gaseous mixture of ethylene and air, composed of oxygen and nitrogen, can be found by the following:

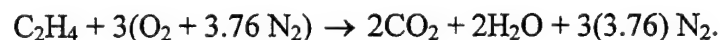$$P_{C_2H_4} = \chi_{C_2H_4}(14.7\,psia), \qquad [3\text{-}2]$$

and
$$P_{air} = \chi_{air}(14.7\,psia). \qquad [3\text{-}3]$$

The term χ is the mole fraction of the molecule or atom and is found by:

$$\chi_{C_2H_4} = \frac{\varphi}{\varphi + (N_{air})_{ST}}, \qquad [3\text{-}4]$$

and
$$\chi_{air} = \frac{(N_{air})_{ST}}{\varphi + (N_{air})_{ST}}. \qquad [3\text{-}5]$$

For example, take the stoichiometric equation for a reaction of ethylene (C_2H_4) and air:

$$C_2H_4 + 3(O_2 + 3.76\,N_2) \rightarrow 2CO_2 + 2H_2O + 3(3.76)\,N_2.$$

27

The sum of the moles of oxidizer is

$3\ O_2 + 3(3.76)\ N_2 = 3$ moles $O_2 + 11.28$ moles $N_2 = 14.28$ moles oxidizer (air),

and the sum of the moles of the fuel is

$1\ C_2H_4 = 1$ mole fuel.

The mole fraction of ethylene is

$$\chi_{C_2H_4} = \frac{1.4}{1.4 + 14.28} = 0.0893 \qquad [3\text{-}6]$$

and the mole fraction of air is 0.9107 by the same method. Therefore, to fill mixing tanks

to 1 atmosphere with a fuel rich $\varphi = 1.4$, the tanks must be filled with 0.0893(14.7 psia)

= 1.31 psia of ethylene and (0.9131)(14.7 psia) = 13.42 psia of air.

7. Data Acquisition

Data acquisition was accomplished by two Microstar data acquisition boards

capable of simultaneous sampling of 8 channels at 800 kHz. A Keithley Metrabyte DAS

1800 board was used to monitor all facility conditions.

High-speed imaging was accomplished using a DRS Hadland Imacon imaging

system. The system can take seven images with a framing rate of up to 100 million

frames per second and a resolution of 532 x 768 pixels.

8. Shock Fence

The shock fence was made of aluminum and machined into a disk that blocked

the outermost 20% of the diameter of the combustion tube. The inner diameter of the

shock fence was 8.130 cm (3.2 in) and the thickness was 0.635 cm (0.25 in).
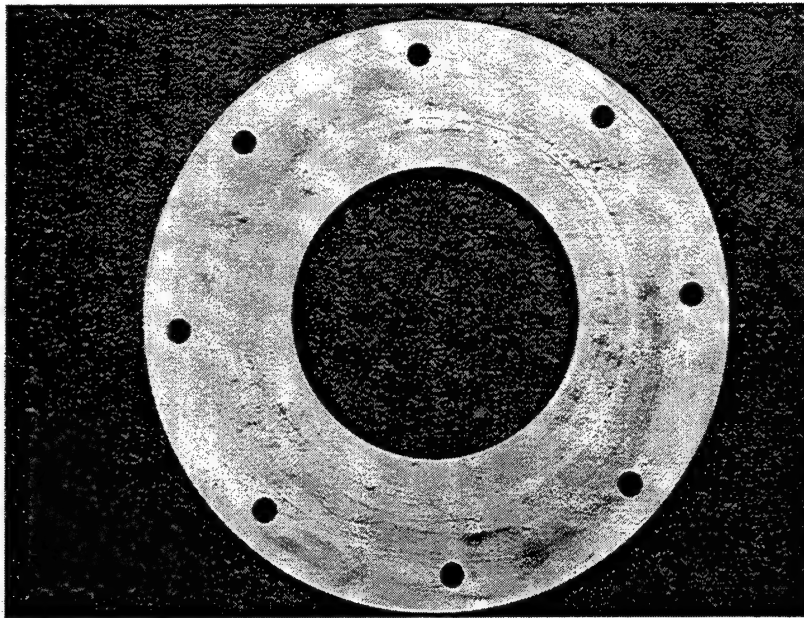
Figure 3-6. Shock Fence With Inner Diameter of 8.128 cm (3.20 in).

9.   Spiral

A spiral, also known as a Schelkin spiral, may be used to increase turbulence along the wall of the combustion tube (Figure 3-7). The spirals used in this testing were made of stainless steel tubing, 0.635 cm (0.25 in) in diameter. The pitch of the spiral was 1 tube diameter (10.2 cm).
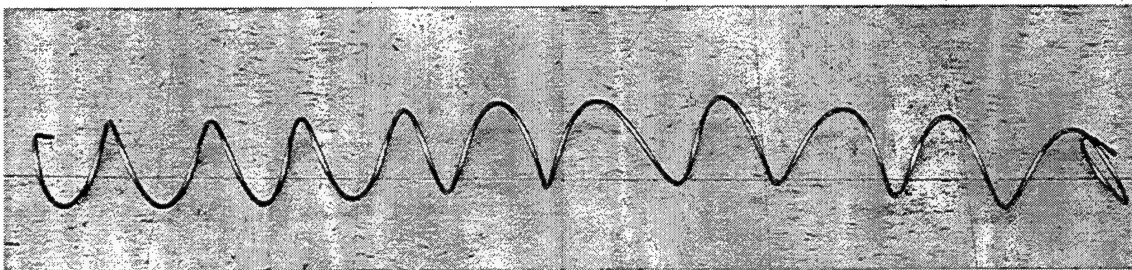

Figure 3-7. Schelkin Spiral. Length is 122 cm.

C.   VARIOUS COMBUSTION TUBE CONFIGURATIONS FOR IMAGING

The optical section was used in three different configurations to aid in imaging. All dimensions in Figures 3-8 through 3-10 are in centimeters. Figure 3-8 shows the optical section set up to image the ignition kernel as it leaves the spark plug. The head-end of this setup can also be seen at the right in Figure 3-2. The camera was triggered by the ignition signal sent to the spark plug. Only one optical port was needed because of the visible light emitted by the combustion event itself. All other ports were covered with aluminum blanks.

Imaging of the orifice plate venting was conducted with the arrangement shown in Figure 3-9. The orifice plate was between the reservoir and the optical section. In this configuration the camera was triggered by a photodiode sensing the light generated by the spark plug discharge in conjunction with a predetermined delay programmed into the camera before the run commenced. This arrangement is also shown in Figure 3-3. The mirror reflecting the image back to the camera is seen in the background.

Shock reflection imaging was conducted near the end of the combustion tube. This setup is shown in Figure 3-10. Camera triggering was accomplished in the same manner as orifice venting imaging using a photodiode. In this case, however, many trials were conducted to determine the correct delay from spark discharge until camera triggering.
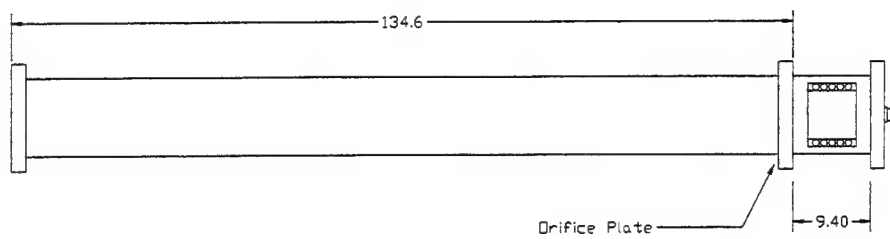
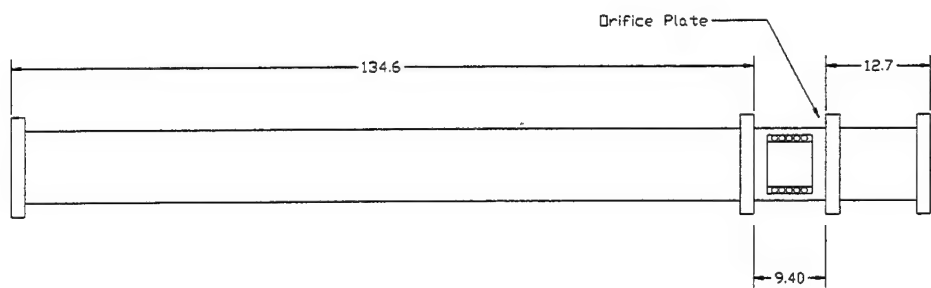Figure 3-8. Setup to image flame kernel growth.
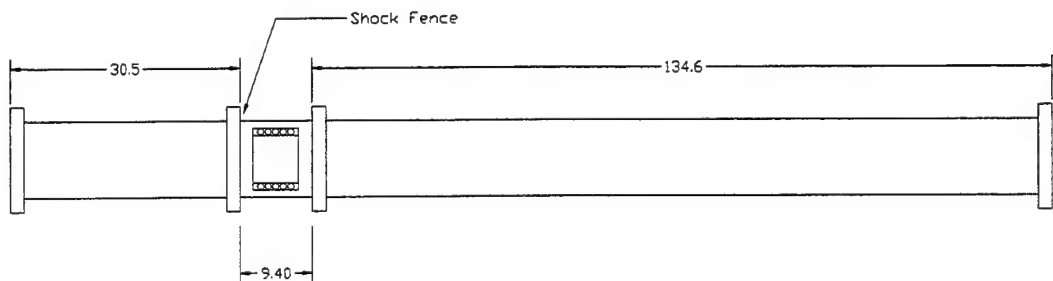

Figure 3-9. Setup to image orifice plate venting.

Figure 3-10. Setup to image shock reflection.

THIS PAGE INTENTIONALLY LEFT BLANK

IV. EXPERIMENTAL RESULTS

A. INTRODUCTION

This research focused on the effects of combustion-tube geometry in three areas: ignition delay time, wave speed, and shock wave reflection. Experiments began with ethylene (C_2H_4) as the fuel because it gives more favorable results in all of the above categories than more complex hydrocarbons.

The ignition delay time, defined later, was measured for various fuel/air mixtures. The results allowed further research to be conducted at the optimum equivalence ratios instead of testing a large range of lean to rich mixtures.

Six orifice-plate geometries with holes of various diameters and numbers were used (Table 3-1). The selection of the best geometry to use in the remainder of the research was based on the pressure rise at the head-end of the reservoir, the rate of venting of combustion products, and the resulting pressure rise observed in the combustion tube.

Experimentally observed wave speeds were compared to theoretically predicted detonation wave speeds for ethylene/air and propane/air mixtures over a range of equivalence ratios predicted from the ignition delay tests. In addition to the orifice plate, a Schelkin spiral was placed against the inner wall of the tube to promote rapid combustion.

Shock wave reflection was examined as a method of thermal initiation for a detonation wave. A shock reflection plate (fence) was used in conjunction with an orifice plate which was used to rapidly generate the incident shock wave.

B. EFFECTS OF TURBULENCE ON COMBUSTION RATE AND WAVE VELOCITY

This research was directed at producing detonations by increasing the turbulent mixing near the wall region. Turbulence dramatically increases the mixing of hot combustion products with cool reactants near the reaction zone resulting in a high overall energy release rate. Figures A-1 and A-2 in Appendix A show the difference a Schelkin spiral makes on the rate of combustion by the dramatic increase of pressure in the combustor. The maximum pressure rise within a tube with no spiral was less than 5 psig (Figure A-1). The tube with a spiral installed produced waves traveling at speeds close to Mach 5 and pressures exceeded 200 psig (Figure A-2).

C. IGNITION DELAY TIME

Ignition delay time was defined as the time after spark discharge it takes for the pressure at the head-end to first exceed 2 psig. The combustion reservoir was partially blocked with an orifice plate and the equivalence ratio was varied to determine the conditions for the fastest chemical reaction. An example of one ignition delay measurement is shown in Figure A-3.

The results shown in Figure A-4 demonstrate the ignition delay time was minimal when the equivalence ratio (φ) was greater than to 1.3 for both fuels. Follow-on testing with the orifice plates using propane was performed at a φ of 1.4 through 1.8 because it was most reactive in this range of equivalence ratios and provided the shortest ignition delay time. Figure A-4 shows that the ignition delay time for ethylene began to rise below a φ of 1.3. Subsequently, follow-on testing with ethylene was done at φ values of 1.4 through 1.8. Values represented in Figure A-4 are averages of many runs.

D. SELECTION OF ORIFICE PLATE GEOMETRY

The orifice plate was one type of combustion enhancement device used in this research. The second phase of this research was to find which geometry provided enough blockage to invoke a fast pressure rise, but still allowed the combustion products to vent rapidly before their heat was quenched by the walls of the tube and orifice plate. Orifice plate geometry selection was based on head-end pressure and the strength of shock generation downstream in the tube.

Combustion was initiated in the reservoir after a spark created an ignition kernel. The ignition kernel was created at the tip of the spark plug and was composed of radicals such as CH, OH, and other ionized species from the breakdown of the fuel/air mixture due to thermal energy deposited from the spark plug. The ignition kernel began moving away from the spark plug, creating a laminar flame front as the fuel/air mixture started to combust from the heat provided by the existing flame. As combustion continued, the flame propagation adjusted itself until a balance was reached between thermal and mass diffusivities. This flame velocity is known as the laminar flame speed.

The sequence of events starting from spark plug discharge and subsequent laminar flame front development can be seen in Figure 4-1. The ignition kernel developed in Figure 4-1 (a) through (c). The fuel/air mixture immediately surrounding the spark plug was ionized and broken down into combustion radicals and other molecules that were extremely reactive. The hot radicals enabled the fuel/air mixture to
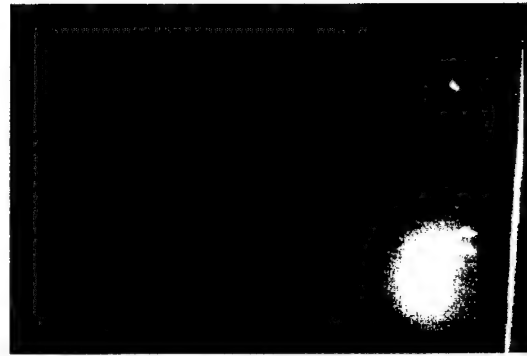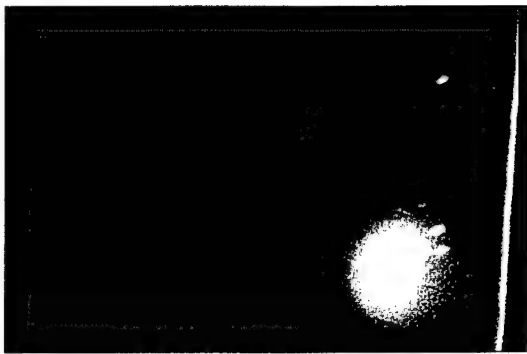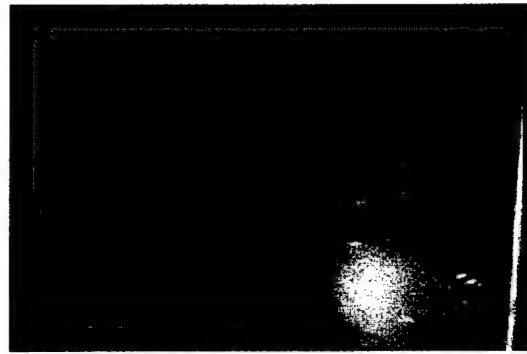
35
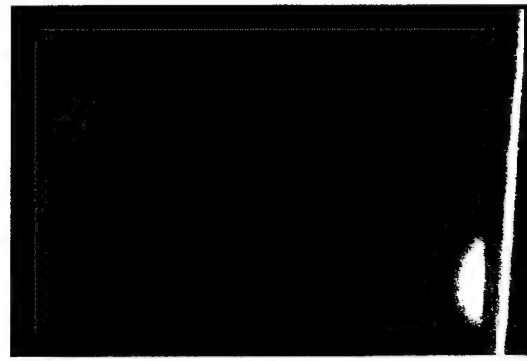
Figure 4-1, (a-f). Flame kernel and subsequent laminar flame front after spark ignition. Exposure time was 250 μs and inter-frame was 1.25 ms.

thermally ignite and the laminar flame front began to move away from the ignition kernel, as shown in Figure 4-1 (d) through (f). The laminar flame front moved toward the orifice plate where large-scale turbulence was created as the flame flowed through the sharp edged holes in the plate.

The testing of the 7-hole orifice plate showed the lack of venting area produced too much flow restriction. The pressure at the head-end of the tube rose sharply, but pressure downstream never rose significantly due to the slow venting and inadequate mixing. The 7-hole plate's performance was similar to the 24-hole Plate 1. The wire mesh produced a pressure rise of almost 40 psig, but did not generate a shock wave.

Figures A-5 through A-8 show the results of the pressure trace for various total venting area for each orifice plate. The equivalence ratio and atmospheric pressure were held constant in each test. Figure A-7 shows the head pressure rose to about 55 psig, but the pressure downstream did not rise past 5 psig. The holes in Plate 1 were too small to allow adequate pressure rise downstream or the venting to take place and the flame was quenched during the slow flow through the orifice plate.

Orifice Plate 2, Figure A-6, vented faster so the head-end pressure rose 13 psig lower than values for Plate 1 and the downstream pressure rose slowly at first, then shot up to 26 psig. Figure A-6 shows the pressure in the head end rose a second time. The second head-end pressure rise was due to the combustion taking place rapidly in the tube at around 0.290 sec on the abscissa. The combustion in the rest of the tube sent pressure waves in all directions, some of which flowed toward the head-end, therefore raising the pressure a second time.

The results for Plates 3 and 4 are compared in Figures A-7 and A-8. Both geometries demonstrated strong shock generation capability. The shocks formed by Plate 3 were stronger with a 50 psig pressure rise. The shocks formed by Plate 4 were formed faster, though not quite as strong as those from Plate 3. The comparison of these two orifice plates shows a trade-off between the two geometries. Plates 3 and 4 were used to further investigate their effect on combustion enhancement when equivalence ratio was varied (Figure A-3).

Figure 4-2 demonstrates the effects on combustion enhancement effects due to the venting jets downstream of the orifice plate at the right of the photograph. The turbulent combustion appears to work its way back to the orifice plate from left to right. However, venting flowed from right to left. The venting, shown in Figures 4-2 (a) and (b), occurred, but the jets are not visible until (c) when the reactants and their products are sufficiently hot to radiate light. Eventually (~10 microseconds) the turbulent, large-scale eddy mixing is sufficient to generate heat and visible flame jets emanating from the orifice plate.
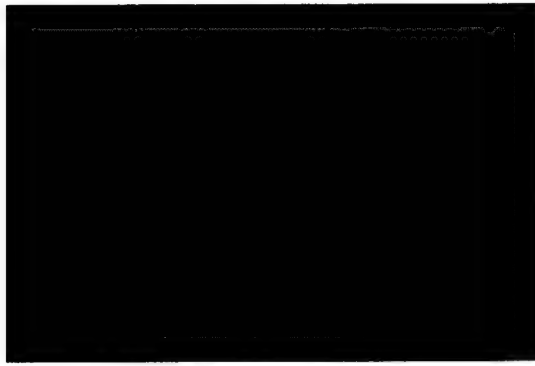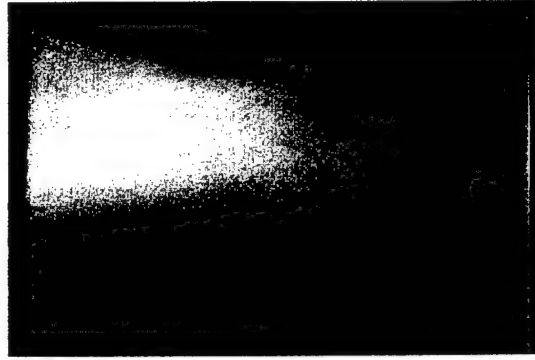
(a)
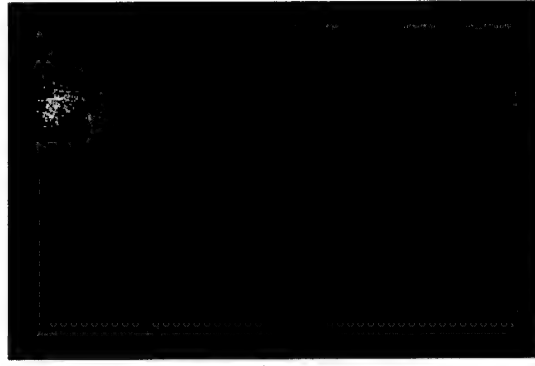
(b)
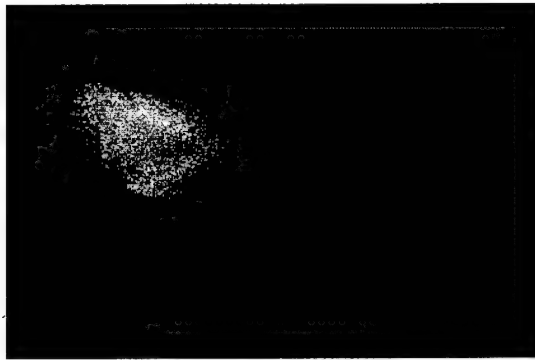
(c)

(d)

(e)

(f)

Figure 4-2, (a-f). View of 24-Hole Orifice Plate venting from right to left. Exposure time was 100 μs and inter-frame time was also 100 μs.

E.   WAVE SPEED

Detonation wave speeds over a range of initial conditions were computed by TEP (Thermodynamic-Equilibrium Program) for ethylene and propane. A good technique to determine if a detonation occurred was to measure its observed wave speed and pressure for comparison with computed detonation properties.

The experimental wave speed was determined from the pressure vs. time plots. Figures A-9 and A-10 demonstrate the method of measuring wave speed. The boxed area in Figure A-9 contains pressure traces of the last 2 pressure transducers. Figure A-10 expands that box and shows 2 pressure peaks from a shock wave passage. The shock wave passed the 2 stations in 165 microseconds, a distance of 0.07509 m, resulting in a wave speed of 455 m/s.

Figures A-11 and A-12 display the experimental and TEP predicted wave speeds for ethylene and propane with various tube geometries. The maximum wave speed for a mixture of ethylene-air at 1 atm occurred between a φ of 1.4 and 1.8 as expected by the ignition delay data trends. Maximum pressures for fully-developed detonations were observed to be about 200-300 psig. Over-driven detonations are the data points in Figure A-11 above the TEP predicted detonation wave speed. The over-driven tests displayed pressures around 500 psig and wave speeds much greater than predicted detonation velocities. Overdriven detonations were due to a series of thermal ignitions between the leading shock wave and the flame front. The unburned reactants in that region were quickly consumed by the explosion and the generated shock waves caused the velocity of the leading shock wave to increase past those at the upper C-J value. The detonation wave formed at that instant shot past the upper C-J point, accelerating through the value

40

for a steady-state detonation wave. The overdriven detonation wave was short lived since flow behind the wave was subsonic and allowed rarefaction waves to propagate to the leading shock and decrease the strength of the overdriven condition. [Ref. 7]

Wave speeds below the TEP prediction line in Figures A-11 and A-12 are quasi-detonations. That is, their wave speed and pressure rise were not high enough to become a detonation wave by the exit of the tube. All of the runs for propane were quasi-detonations. The test runs with propane and the spiral and orifice plate geometry were within 100 m/s at a φ of 1.5 to 1.6 of deflagration-to-detonation transition.

Since the overall reaction rate was slower, it was more difficult to produce a detonation at the same conditions as ethylene. The results, however, did follow the trend showed by the ethylene testing. The wave speeds were highest when both the orifice plate and the spiral were used together. The next fastest waves were produced by the spiral, followed by the orifice plate geometry.

F. SHOCK REFLECTION

Results of a shock reflection test are shown in Figure A-13. A portion of the shock wave was forced to reflect upon itself and further increase the temperature and pressure of the reactants. Runs were conducted at various equivalence ratios but only produced quasi-detonations. The initial temperature of 350 K was not high enough to reach auto-ignition temperatures after shock wave reflection, around 900 K for these hydrocarbons. Additional heaters and insulation were needed to increase the initial temperature. The initial temperature of the tube and reactants needs to be about 450 K to attain auto-ignition temperature

41

G. ORIFICE PLATE IMPROVEMENT

The images in Figure 4-2 showed that the flow, after orifice plate venting, is drawn toward the center because of the lower pressure induced along the centerline from the strong venting taking place from the inner-ring of holes. A more planar venting structure was desired to create turbulence equally throughout the combustion tube cross-section.

An orifice plate with 12 holes positioned toward the outer diameter of the plate was constructed to force the venting to occur in the area near the tube wall and then spread through eddy circulation to the centerline. Results with ethylene/air mixtures have shown improvement over the previous 24-hole orifice plate design. The rapid turbulence mixing took place 5 times faster with the new orifice plate design. The newly designed 12-hole plate required 50 µs from orifice venting to visible flames reaching the head-end of the tube (Figure 4-3, a-c). The 24-hole plate took 500 µs for the same event to occur. Figure 4-3 (b) and (c) show that the turbulent mixing took place in a more planar structure. Testing was not conducted with a propane/air mixture because of time constraints.

(a)

(b)
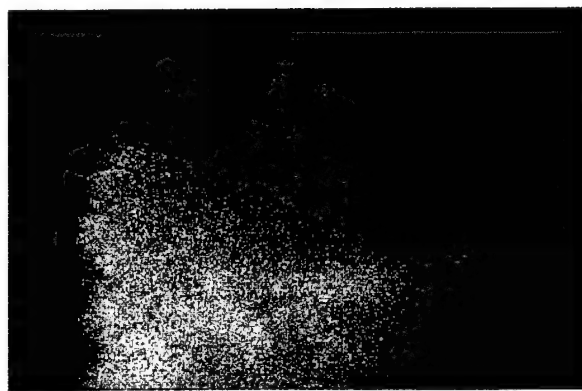
(c)

Figure 4-3 (a-c). 12-Hole Orifice Plate Venting.
Exposure time was 10 μs and inter-frame time was 20 μs.

THIS PAGE INTENTIONALLY LEFT BLANK

V. CONCLUSIONS

A. SUMMARY

The range of optimum equivalence ratios for maximum detonation wave speed found by the ignition delay tests was consistent with the range most often utilized in reported PDE investigations. The maximum wave speeds occurred in the range of $\varphi =$ 1.4 to 1.8. The multi-hole orifice plate provided improvement in pressure rise and wave speed compared to a clean tube for both propane/air or ethylene/air mixtures, but did not provide a detonation. The Schelkin spiral increased the maximum wave speed by almost 1000 m/s for ethylene and 600 m/s for propane compared to orifice plate results, but again did not provide a detonation. Finally, the fastest wave speeds and highest pressures were achieved with the spiral and orifice plate used concurrently, reliably producing a detonation with an ethylene/air mixture. Detonations were not produced, however, with propane using the same geometry. Trends with propane did follow those observed with ethylene.

The fence, which provided partial shock reflection, produced quasi-detonations with both fuels. It was determined that a higher initial temperature of approximately 450K would be required to reach the auto ignition temperature of about 900K using this technique and subsequently increase the probability of detonation wave generation. Additional heating elements will be needed to attain proper initial temperatures.

Imaging of the combustion jets venting through the orifice plate showed that the orifice geometry needs further optimization. The curved flame front reached the inner orifice circle first and caused venting near the centerline of the plate before the outer

circle of holes began to vent. The inner ring of jets lowered the pressure along the centerline, drawing the outer jets toward the center. To get the maximum effect of turbulent mixing, the venting needs to possess a more planar structure.

This work has shown that combustion enhancing geometries created turbulence and increased the combustion rate to achieve higher pressures and wave speeds in a combustion tube. Detonations using ethylene/air mixtures were detonated in less than 1 meter and propane/air mixtures showed marked improvement over clean tube configurations when combusted with the orifice plate/spiral combination installed in the combustion tube.

B.   RECOMMENDATIONS

It is hoped that propane could produce detonation waves in less than 1 meter when combusted with the 12-hole plate design that created a planar venting structure when tested with ethylene/air mixtures. Time did not permit this orifice plate to be tested with propane. Further testing with propane/air mixtures is warranted.

APPENDIX A.   FIGURES A-1 THROUGH A-12

The following figures supplement the results and are referred to in this research.

All measured wavespeeds have an error of +/- 73 m/s. All time measurements have an
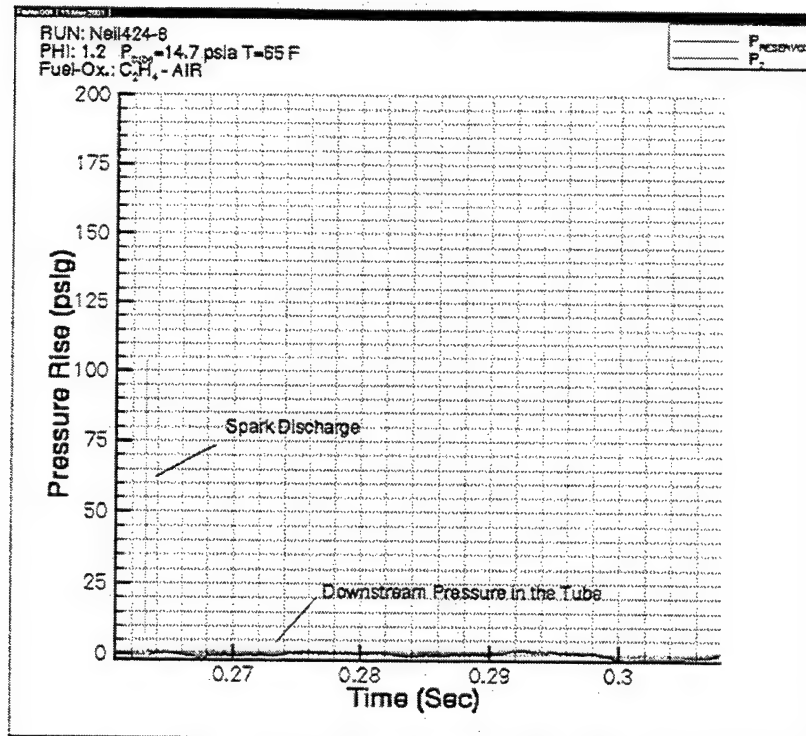
error of +/- 1.6μs .
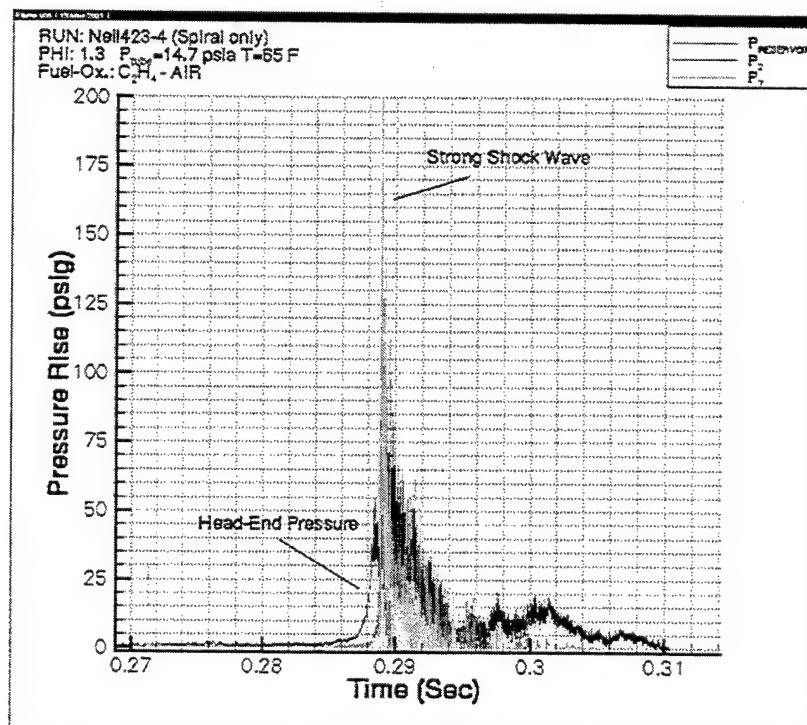
Figure A-1. Clean Combustion Tube.
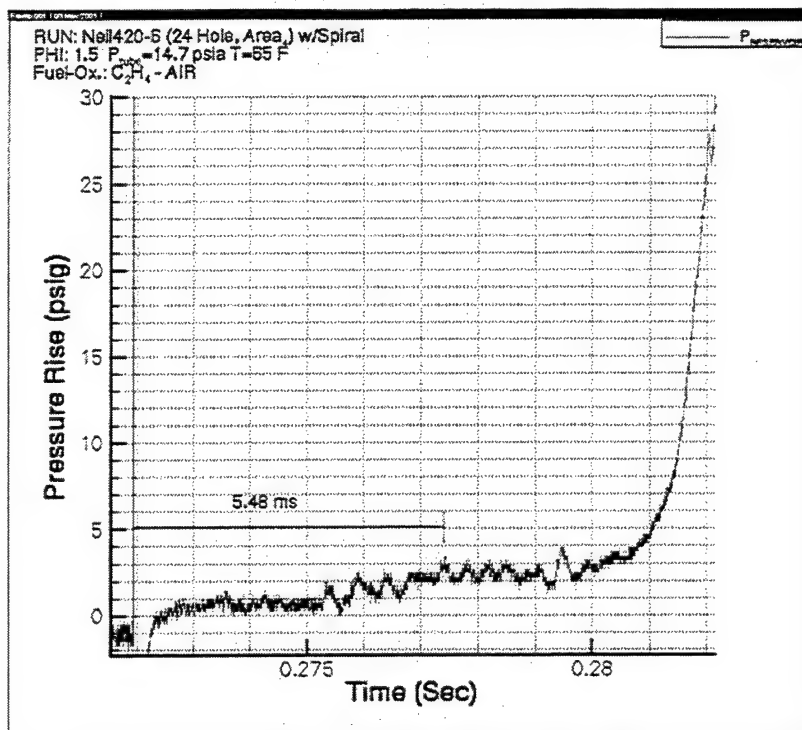

Figure A-2. Combustion Tube with Spiral.

48

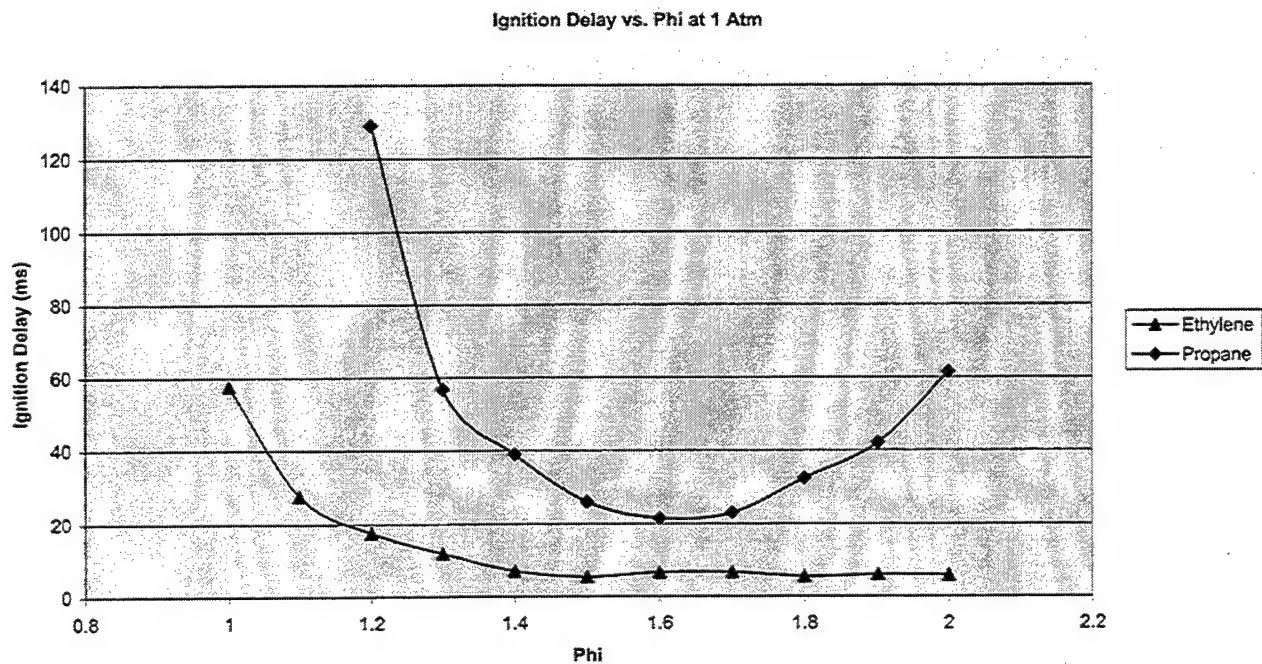Figure A-3. Measurement of Ignition Delay Time for Ethylene/Air Mixture.

Figure A-4. Ignition Delay Time vs. Phi for Ethylene and Propane.
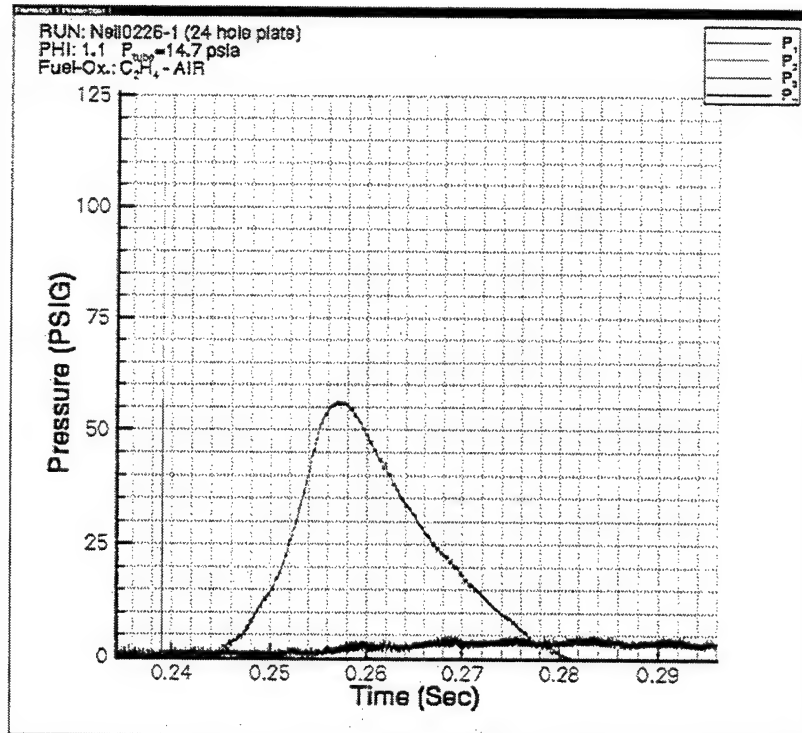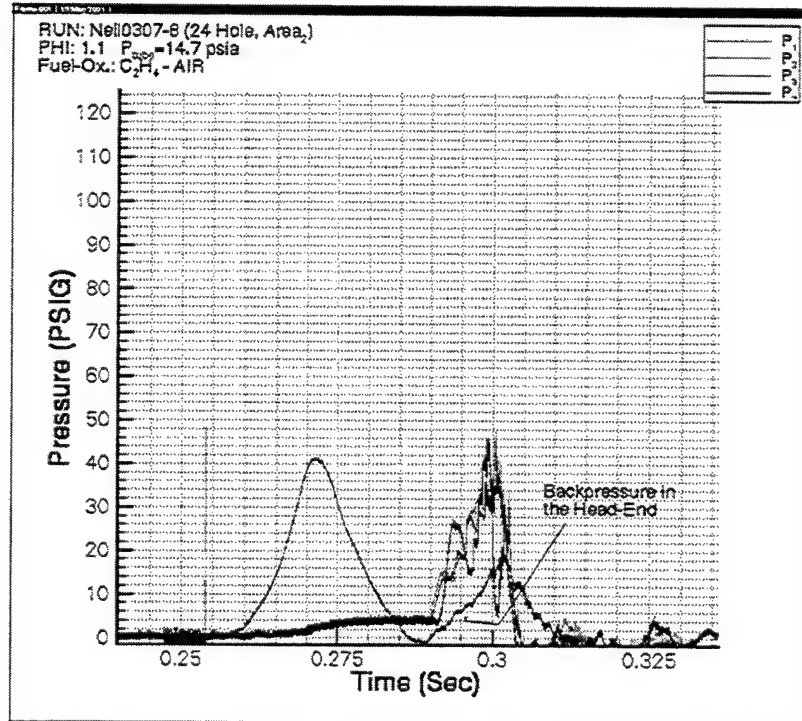
Figure A-5. Orifice Plate 1.
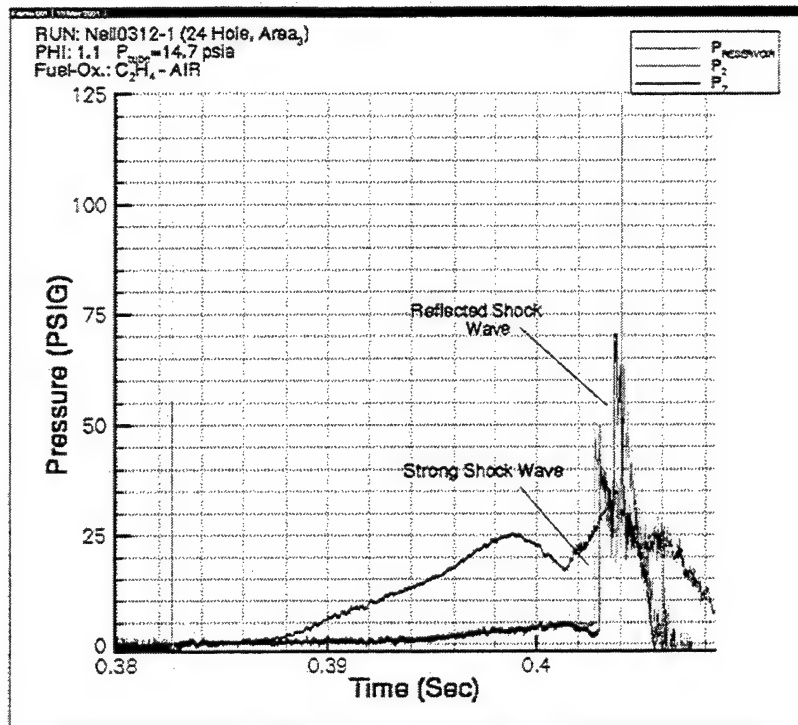

Figure A-6. Orifice Plate 2.

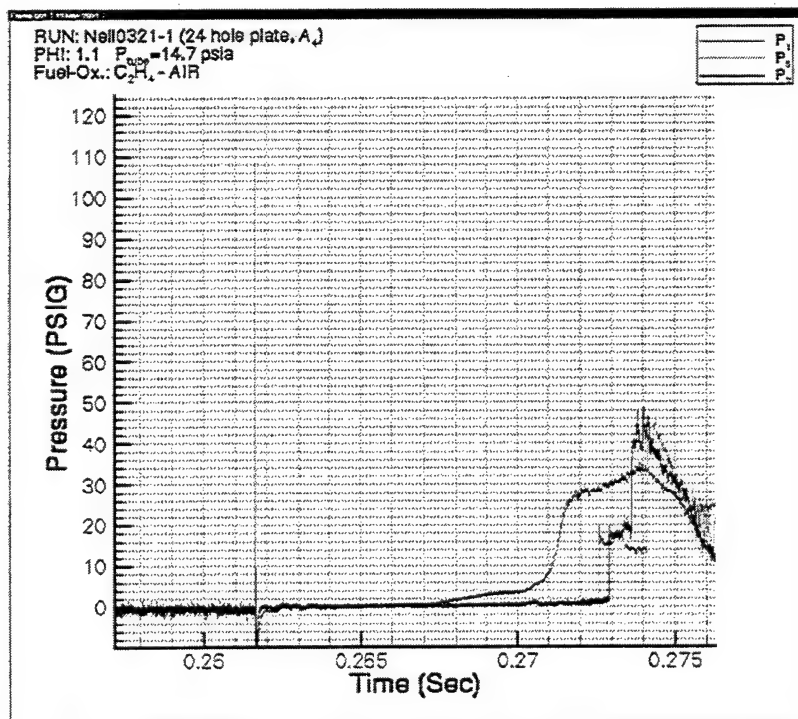Figure A-7. Orifice Plate 3.

Figure A-8. Orifice Plate 4.
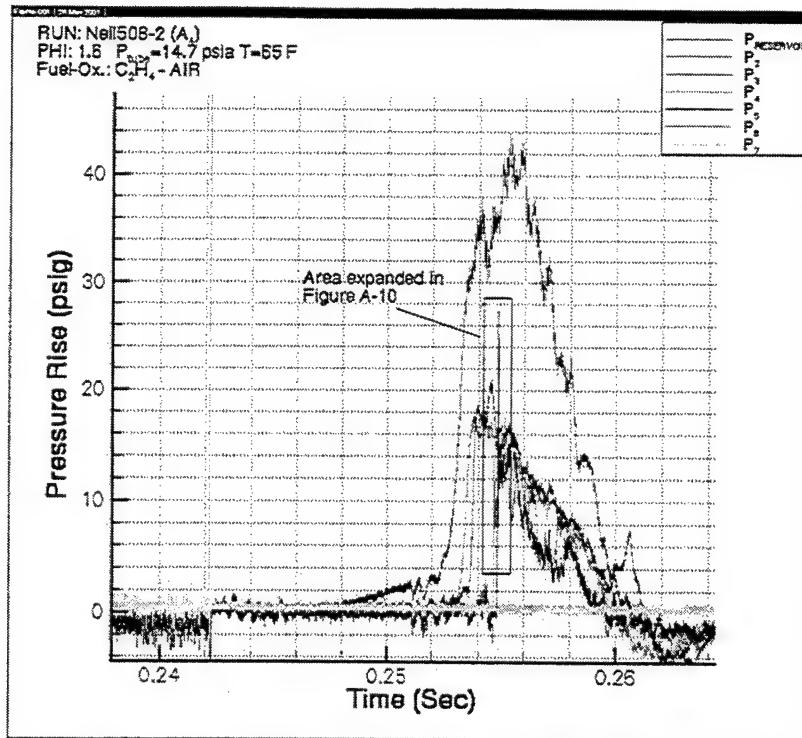
Figure A-9. Boxed Area Expanded in Figure A-10 to Measure Wave Speed.
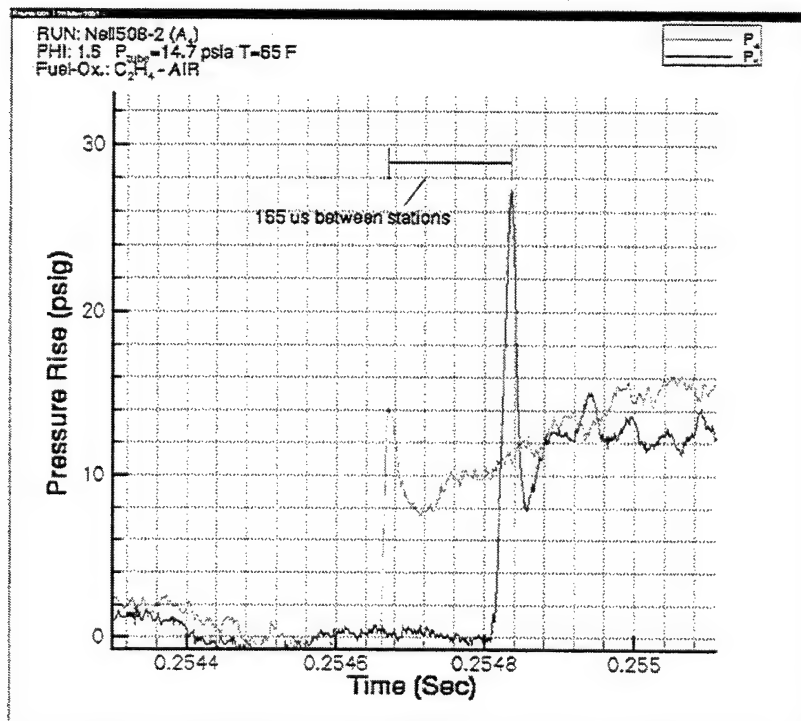

Figure A-10. Time Elapsed for Shock Wave Passage between 2 Pressure Sensors. Error in time measurement is +/- 1.6 μs.
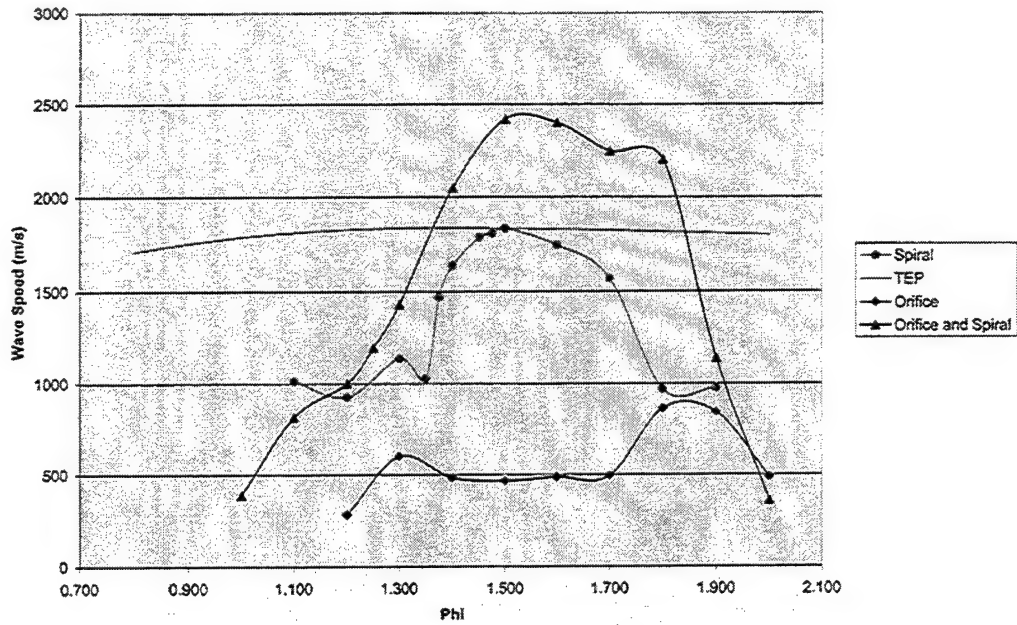
Figure A-11. Wave Speeds for Ethylene with Various Geometries.
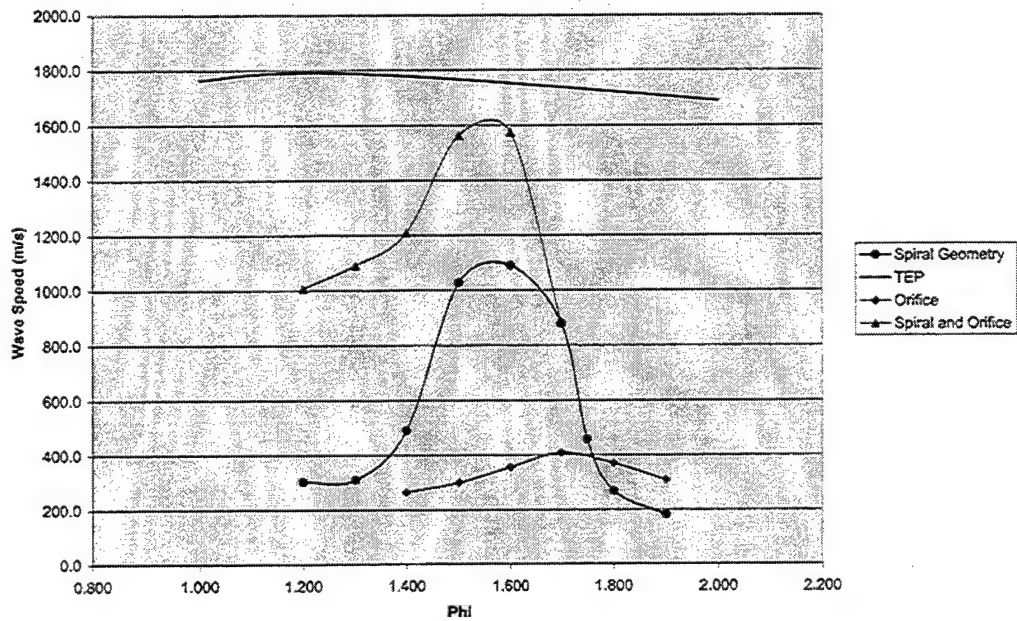Wave speed error is +/- 73 m/s.

Figure A-12. Wave Speed for Propane with Various Geometries.
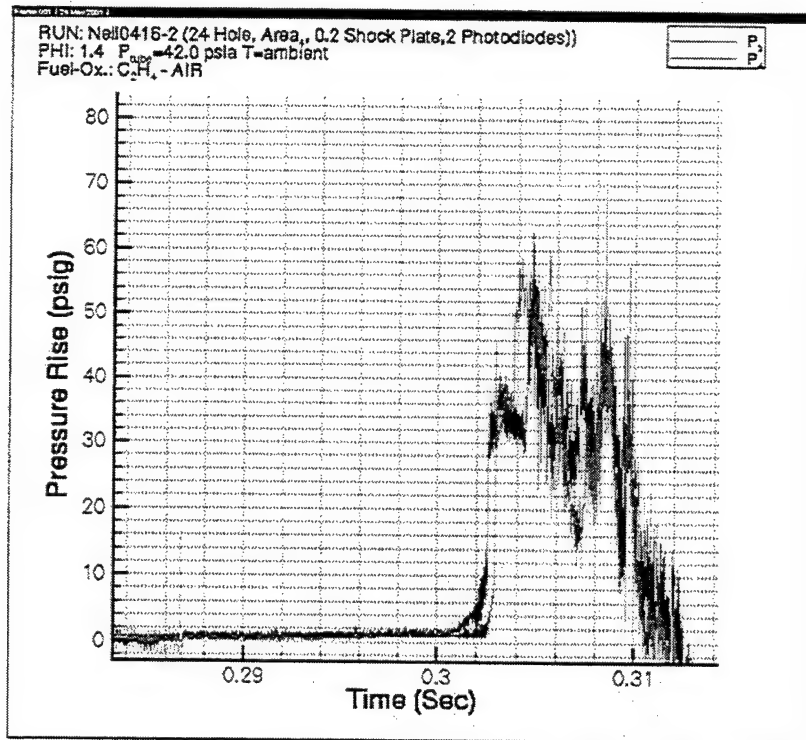Wave speed error is +/- 73 m/s.

Figure A-13. Shock Wave Reflection with a Fence Installed.

TEST CELL 1: 4" SINGLE PULSE DETONATOR

Standard Operating Procedure

Open Facility Procedure
1) Verify "Emergency Shutdown" switch is pushed IN.
2) Turn on 24 VDC and 115 VAC power supply to cell 1.
3) Turn on yellow "compressed gas present" warning lights.
4) Turn on Kistler electronics, set to proper gain, and set to Operate mode.
5) Open 'shop air' actuator air line.
6) Enable capacitor discharge ignition system.
7) Open ethylene or propane gas bottle and set supply pressure.
8) Ensure air bottles are aligned and contain sufficient pressure to support operations.
9) Turn on video camera and other data recording equipment as necessary.

Run Mode
10) Enter 'Jet Ignition' Visual Basic program on Boomer computer.
11) Reset Emergency Shutdown switch.
12) Go to 'Run Conditions' and set proper equivalence ratio, atmospheric pressure, mixing tank pressure, and mixing time.
13) Go to 'Open Facility' and 'Enable Manual Control'.
14) Notify Lab personnel that a run is about to commence.
15) Press 'Start Run' and ensure that tube is being evacuated.
16) Acknowledge 'Tube Ready' after program has evacuated tube and filled mixing tank for allotted time.
17) When golfers are clear, start siren.
18) Begin recording VCR.
19) Enable 'Fire' and 'Data Acquisition' buttons.
20) After final safety check for Lab personnel and golfers, press 'Fire/Open' button.
21) After test run, turn off siren and stop recording on VCR.
22) Ensure file name is typed in and then press 'Save Data' button.
23) After completion of each run, open 'Vent Valve' to vent mixing tank.
24) Upon completion of data collection, press 'Close Facility'

Figure A-14. Standard Operating Procedure for the Single Pulse Detonator.

THIS PAGE INTENTIONALLY LEFT BLANK

LIST OF REFERENCES

1. Robinson, John P., *Influence of Ignition Energy, Ignition Location, and Stoichiometry on the Deflagration-to-Detonation Distance in a Pulse Detonation Engine*, Master's Thesis, Naval Postgraduate School, Monterey, California, June 2000.

2. Glassman, I.G., *Combustion*, Academic Press Inc., 1987.

3. Teodorczyk, A., Lee, J.H.S., Knystautas, R., "Photographic Study of the Structure and Propagation Mechanisms of Quasidetonations in Rough Tubes", *Dynamics of Detonations and Explosions: Detonations,* AIAA, 1990.

4. Frolov, S.M., Gelfand, B.E., Medvedev, S.P., "Calculation of the Velocity of Gaseous Detonation in a Rough Tube Based on Measurements of Shock Wave Attenuation", *Dynamics of Detonations and Explosions: Detonations,* AIAA, 1990.

5. Beeson, H.D., McClenagan, R.D., Bishop, C.V., Benz, F.J., "Detonability of Hydrocarbon Fuels in Air", *Dynamics of Detonations and Explosions: Detonations,* AIAA, 1990.

6. Bauer, P.A., Dabora, E.K., Manson, N., "Chronology of Early Research on Detonation Wave", *Dynamics of Detonations and Explosions: Detonations,* AIAA, 1990.

7. Kuo, K. K., *Principles of Combustion*, John Wiley & Sons, 1986.

8. Zucker, R.D., *Fundamentals of Gas Dynamics,* Matrix Publishers Inc., 1977.

9. Murray, S.B., Moen, I.O., Thibault, P.A., "Initiation of Hydrogen-Air Detonations by Turbulent Fluorine-Air Jets", *Dynamics of Detonations and Explosions: Detonations,* AIAA, 1990.

THIS PAGE INTENTIONALLY LEFT BLANK

INITIAL DISTRIBUTION LIST

1. Defense Technical Information Center..2
    8725 John J. Kingman Rd., STE 0944
    Ft. Belvoir, VA 22060-6218

2. Dudley Knox Library Center...2
    Naval Postgraduate School
    411 Dyer Rd.
    Monterey, CA 93943-5101

3. Curriculum Office, Code 34 1
    Mechanical Engineering Department
    Naval Postgraduate School
    Monterey, CA 93943-5000

4. Dr. Christopher M. Brophy, Code AA/Br...3
    Department of Aeronautics and Astronautics
    Naval Postgraduate School
    Monterey, CA 93943-5000

5. Dr. James V. Sanders...1
    Physics Department
    Naval Postgraduate School
    Monterey, CA 93943-5000

6. Dr. David W. Netzer, Code AA/Nt..1
    Department of Aeronautics and Astronautics
    Naval Postgraduate School
    Monterey, CA 93943-5000

7. Dr. William B. Maier, Code PH/Mw..1
    Physics Department
    Naval Postgraduate School
    Monterey, CA 93943-5000

8. LT Neil G. Sexton...2
    7120 Patronis Drive, Apt 2008
    Panama City Beach, FL 32408

9. Dr. Gabriel Roy...1
    Office of Naval Research
    Mechanics Division, Office 333
    Ballston Tower One
    800 N. Quincy Street
    Arlington, VA 22217-5660

Physics Department
Naval Postgraduate School
Monterey, CA 93943-5000